

# Photophysical Properties of Organogold(I) Complexes Bearing a Benzothiazole-2,7-Fluorenyl Moiety: Selection of Ancillary Ligand Influences White Light Emission

Joseph J. Mihaly,<sup>a</sup> David J. Stewart,<sup>b,c</sup> Tod A. Grusenmeyer,<sup>b</sup> Alexis T. Phillips,<sup>b,d</sup> Joy E. Haley,<sup>b</sup> Matthias Zeller,<sup>e</sup> and Thomas G. Gray<sup>a,\*</sup>

<sup>a</sup>Department of Chemistry, Case Western Reserve University, 10900 Euclid Avenue, Cleveland, Ohio 44106, United States

<sup>b</sup>Air Force Research Laboratory, Materials and Manufacturing Directorate, Wright-Patterson Air Force Base, Dayton, Ohio 45433, United States

<sup>c</sup>General Dynamics Information Technology, 5100 Springfield Pike, Dayton, Ohio, 45431, United States

<sup>d</sup>Southwestern Ohio Council for Higher Education, Dayton, Ohio, 45420, United States

<sup>e</sup>Department of Chemistry, Purdue University, West Lafayette Indiana, 47907, United States

## Table of Contents:

I.	Materials and Methods	S2-S7
II.	Synthesis, NMR, Mass Spectrometry and Elemental Analysis	S8-S15
III.	Supplemental Figures	S16-S23
IV.	Calculations	S24-S32
V.	X-ray Crystallography	S33-S36
VI.	References	S37-S38

## II. Materials and Methods

**General Considerations.** All experimental procedures were carried out under an inert atmosphere of argon using standard Schlenk line techniques. Microanalyses (C, H, and N) were undertaken by Midwest Microlab and Atlantic Microlab. Mass spectrometry was performed at the University of Cincinnati Mass Spectrometry facility. (Phosphine)gold(I) chloride and (*i*-Pr<sub>2</sub>NHC)AuCl were prepared according to literature procedures.<sup>1</sup> The corresponding gold(I) bromides were prepared by reacting one equivalent of gold(I) chloride with five equivalents of potassium bromide in a 1:1 mixture of DCM/Water, extraction in DCM yielded the bromides quantitatively. 2-(9,9-Diethyl-7-(4,4,5,5-tetramethyl-1,3,2-dioxaborolan-2-yl)-9*H*-fluoren-2-yl)benzo[*d*]thiazole was purchased from Synovel Labs. Dry 2-propanol, benzene, dichloromethane, pentane, and cesium carbonate was purchased from Sigma Aldrich and used as received. <sup>1</sup>H NMR experiments were performed on a Bruker-500 Ascend Advanced III HD NMR spectrometer operating at 500.24 MHz. All NMR experiments were run at a millimolar concentration. <sup>1</sup>H chemical shifts are reported in parts per million ( $\delta$ ) with integration and multiplicity (s = singlet, d = doublet, t = triplet, q = quartet, dd = doublet of doublets, dt = doublet of triplets, td = triplet of doublets, ddd = doublet of doublet of doublets, and m = multiplet), measured from tetramethylsilane (0 ppm) and are referenced to residual solvent in CDCl<sub>3</sub> (7.26 ppm). <sup>31</sup>P{<sup>1</sup>H} NMR, chemical shifts were determined relative to concentrated H<sub>3</sub>PO<sub>4</sub>.

**Instrumentation.** Ground-state UV/vis absorption spectra were measured using a Cary 5000 spectrophotometer. Visible luminescence spectra were obtained using an Edinburgh Instruments FLS980 spectrometer. The samples were excited using a 450 W xenon lamp attached to a Czerny-Turner monochromator (300 nm focal length, 1800 grooves/mm grating, 1.8 nm/mm linear dispersion). The emission signal is collected at 90° relative to the excitation source and passed through a Czerny-Turner monochromator (300 nm focal length, 1800 grooves/mm grating, 1.8 nm/mm linear dispersion) prior to being collected with a Hamamatsu R928P side window photomultiplier in a cooled housing (Operating temperature: -20 °C). The CIE 1931 chromaticity diagram was generated using the Chromaticity Diagram app in the Origin software. 77K luminescence spectra were collected using the visible luminescence setup described above. The samples were frozen in a dewar filled with liquid nitrogen prior to being lowered into the sample chamber. NIR luminescence spectra were obtained using the same excitation source and monochromators, but with a Hamamatsu R5509-72 Photomultiplier in a nitrogen-flow cooled housing (Operating temperature: -80 °C). Luminescence lifetimes were collected using an Edinburgh Instruments OB920 spectrometer. The fluorescence lifetimes were determined using time-correlated single-photon counting. The samples were excited using a 375 nm pulsed LED source with a pulse duration of 60 ps. The fluorescence signal was observed at 415 nm for all samples. Reconvolution fits of the fluorescence decay

traces and the IRF were completed using the Edinburgh Instruments F900 software package. The phosphorescence lifetimes were collected using multi-channel scaling. The samples were excited using a pulsed xenon flashlamp with a 1.2  $\mu$ s pulse width and an average power of 60 W attached to a Seya-Namioka monochromator (100 nm focal length, 1200 grooves/mm grating). The samples were all excited at 348 nm and the phosphorescence signal was observed at 540 nm. The decay traces were fit using monoexponential decay kinetics. Prior to the collection of the phosphorescence lifetime data, the samples were deaerated with three freeze-pump-thaw cycles. The final achieved vacuum pressure is included with lifetime data. All lifetime measurements were collected in duplicate. The lifetime fits and residuals for the fluorescence and phosphorescence decays are shown in Figure S10.

Nanosecond transient absorption and delayed fluorescence measurements were performed using an Edinburgh Instruments LP920. Samples were excited using the frequency tripled output (355 nm) of a Q-switched Nd:YAG laser (Quantel Vibrant, pulse width approximately 5 ns). Transient absorption spectra were collected using an Andor iStar ICCD camera. Transient absorption kinetics were collected using a Hamamatsu R928 PMT and a Tektronix TDS 3012C Digital Storage Oscilloscope. Electronic synchronization was controlled via the Edinburgh Instruments F900 software package. Laser excitation of the samples was aligned 90° relative to the white light probe. For single-wavelength kinetic measurements, the probe entered a Czerny-Turner monochromator (300 nm focal length, 1800 grooves/mm grating, 1.8 nm/mm linear dispersion) before being passed to the PMT. For transient absorption spectra, the image from the grating was imaged onto the ICCD camera. The delayed fluorescence and triplet-triplet annihilation experiments were collected using the freeze-pump-thaw degassed samples used for the collection of the phosphorescence lifetimes. Excited-state extinction coefficient measurements were collected in aerated toluene solution.

Ultrafast transient absorption measurements were performed using a modified version of the femtosecond pump-probe UV-Vis spectrometer described elsewhere.<sup>12</sup> Briefly, 4 mJ, 45 fs pulses at 785 nm with a 1 kHz repetition rate were obtained from a cryogenically-cooled Ti:Sapphire regenerative amplifier (KM Labs Wyvern 1000-10). Approximately 5% (0.2 mJ) was reflected into the experiment, which was split into pump and probe (90% and 10%, respectively) using a beam splitter. The pump beam was directed into a frequency doubler (CSK Super Tripler) and then focused into the sample. The probe beam was delayed in a computer-controlled optical delay (Newport MM4000 250 mm linear positioning stage) and then focused into a sapphire plate to generate white light continuum. The white light was then overlapped with the pump beam in a 2 mm quartz cuvette and then coupled into a CCD detector (Ocean Optics S2000 UV-VIS). Data acquisition was controlled by software developed by Ultrafast Systems LLC. Global analysis of the lifetime of each chromophore at 10 unique wavelengths was also performed with the Ultrafast Systems LLC Surface Explorer software package. All of the decays are fit well with monoexponential decay kinetics. The value

represented in Table 1 is the average of this global lifetime analysis. The fit and residuals obtained from the fit at a single wavelength are shown in Figure S17. All ultrafast data were collected in aerated toluene solutions.

**Absolute Luminescence Quantum Yield Measurements.** Fluorescence quantum yield values were determined using an integrating sphere compatible with the Edinburgh Instruments FLS980 system. A detailed discussion of collecting and determining absolute quantum yields using an integrating sphere is described elsewhere.<sup>13</sup> The excitation intensity was set by placing a blank toluene solution into the sample chamber. The emission slits were set to 0.8 mm and the excitation slits (5 mm) were adjusted until 1 million counts were observed at the PMT. All of the samples were excited at 300 nm. The luminescence signal was collected from 280 – 600 nm using a 0.3 nm step size. The luminescence signal was averaged 3 times for each trial. Each quantum yield was collected in duplicate. The fraction of light absorbed was determined by integrating the excitation signal of the blank sample and the excitation signal obtained from the particular AuBTF sample and subtracting the values. The excitation signal was integrated from 295 - 305 nm. The raw fluorescence intensity signal was integrated from the crossing point of the toluene blank signal and the AuBTF sample signal to 600 nm. The raw fluorescence intensity spectra were corrected for sample reabsorption. The concentrated samples had a ground state absorbance value of 0.1 at 310 nm. The concentrated samples were diluted by a factor of 10 and the emission spectra were recollected in order to determine the extent of reabsorption loss. The data used to determine the fluorescence quantum yield values for all of the AuBTF complexes is show in Figure S11.

**Relative Luminescence Quantum Yield Measurements.** The phosphorescence quantum yield values for the AuBTF complexes and photosensitized singlet oxygen phosphorescence quantum yield values in aerated samples of the AuBTF complexes were determined using relative quantum yield measurements. A discussion of relevant luminescence quantum yield standards<sup>14</sup> and detailed overview of the collection of relative quantum yield measurements<sup>15</sup> are summarized elsewhere. The equation used to determine the luminescence quantum yield of a sample using a reference standard is given below in equation 1.

$$(1) \quad \Phi_{f,x} = \Phi_{f,std} \frac{F_x}{F_{std}} \frac{f_{std}(\lambda_{ex,std})}{f_x(\lambda_{ex,x})} \frac{\eta_x^2}{\eta_{std}^2}$$

$\Phi_{f,std}$  is the luminescence quantum yield of the reference standard,  $F_x$  and  $F_{std}$  are the integrated luminescence intensity values obtained from the unknown and reference standard,  $f_x(\lambda_{ex,x})$  and  $f_{std}(\lambda_{ex,std})$  represent the fraction of light absorbed by the unknown and reference standard, and  $\eta_x^2$  and  $\eta_{std}^2$  are the indices of refraction for the solvents used to collect the luminescence spectra of the unknown and reference. The index of fraction correction is only applied in instances when the solvent used to collect the luminescence spectra of the unknown and reference differ. The phosphorescence quantum yields for the AuBTF

complexes were determined using Rhodamine 6G as the reference standard. The samples were absorbance matched at 348 nm. The samples were excited using an excitation slit width of 1.25 mm. The luminescence signal was collected from 450 – 700 nm using 1 nm steps with an emission slit width of 0.50 mm. The luminescence signal was averaged 5 times for each trial. The phosphorescence spectra were integrated from 500 – 750 nm. The phosphorescence quantum yield experiments were performed in duplicate for AuBTF0 and AuBTF1 and in triplicate for AuBTF2. The AuBTF luminescence spectra were collected in toluene. The Rhodamine 6G luminescence spectrum was collected in EtOH. The equation was corrected using the index of refraction values reported in the Handbook of Photochemistry.<sup>16</sup> The ground-state absorption correction for the AuBTF and Rhodamine 6G samples used the average absorption value from 347 – 349 nm to account for the linear dispersion of the excitation monochromator. The luminescence spectra of Rhodamine 6G was corrected for reabsorption. A quantum yield value of 0.95 was applied to the integrated intensity of the corrected luminescence spectrum of Rhodamine 6G.<sup>14</sup> The absorption and luminescence data used to determine the phosphorescence quantum yields of the AuBTF complexes are shown in Figure S12. The photosensitized singlet oxygen phosphorescence quantum yields for the AuBTF complexes were determined using phenazine as the reference standard.<sup>17</sup> The reference and AuBTF luminescence spectra were collected in benzene. The samples were absorbance matched at 361 nm. The samples were excited using an excitation slit width of 3.0 mm. The luminescence signal was collected from 1240 – 1330 nm using 1 nm steps with an emission slit width of 21.0 mm. The luminescence signal was averaged 50 times for each trial. The singlet oxygen phosphorescence spectra were integrated from 1250 – 1320 nm. The ground-state absorption correction for the AuBTF and phenazine samples used the average absorption value from 359 - 363 nm to account for the linear dispersion of the excitation monochromator. A quantum yield value of 0.88 was applied to the integrated intensity of the photosensitized singlet oxygen phosphorescence from the phenazine reference sample.<sup>17</sup> The phosphorescence quantum yield experiments were performed in duplicate for all of the AuBTF complexes. The absorption and luminescence data used to determine the singlet oxygen phosphorescence quantum yields are shown in Figure S13.

**Triplet Excited-State Extinction Coefficient Determination.** The excited-state extinction coefficients of the AuBTF triplet states were determined using a relative actinometry method with [Ru(bpy)<sub>3</sub>]<sup>2+</sup> as a standard. Standard methods for the determination of the excited-state extinction coefficients and the tabulation of the triplet-triplet absorption spectra of a multitude of molecules are presented elsewhere.<sup>18</sup> The equation used to determine the excited-state extinction coefficient of a sample using a reference standard is given below in equation 2.

$$(2) \quad \Delta\varepsilon_{T,\lambda} = \frac{\Delta\varepsilon_{Ru,\lambda}(\Delta A_{X,\lambda}/\Delta A_{Ru,\lambda})}{\Phi_T} \frac{\eta_X^2}{\eta_{Ru}^2}$$

$\Delta\epsilon_{\text{Ru},\lambda}$  is the difference between the excited- and ground-state extinction coefficients of  $[\text{Ru}(\text{bpy})_3]^{2+}$  at a particular wavelength,  $\Delta A_{\text{x},\lambda}$  is the absorbance change at a particular wavelength of the unknown compound following laser excitation,  $\Delta A_{\text{Ru},\lambda}$  is the absorbance change at a particular wavelength of  $[\text{Ru}(\text{bpy})_3]^{2+}$  following laser excitation,  $\phi_{\text{T}}$  is the intersystem crossing efficiency for the unknown sample, and  $\eta_{\text{x}}^2$  and  $\eta_{\text{Ru}}^2$  are the indices of refraction of the solvents used to collect the transient absorption traces of the unknown sample and  $[\text{Ru}(\text{bpy})_3]^{2+}$ . The  $[\text{Ru}(\text{bpy})_3]^{2+}$  reference sample and the AuBTF samples were absorbance matched and excited at 355 nm. A value of  $20,800 \text{ M}^{-1}\text{cm}^{-1}$  was used as the value of  $\Delta\epsilon_{\text{Ru},\lambda}$  at 370 nm in  $\text{CH}_3\text{CN}$ . This value is based on the literature value for the excited-state extinction coefficient in water at 364 nm<sup>19</sup> of  $25,400 \text{ M}^{-1} \text{ cm}^{-1}$  and a ground-state extinction coefficient of  $4,600 \text{ M}^{-1} \text{ cm}^{-1}$  at 364 nm determined in our laboratory. It is assumed the  $\Delta\epsilon$  value at the maximum in water (364 nm) is equal to the value at the maximum in  $\text{CH}_3\text{CN}$  (370 nm). The value of  $\phi_{\text{T}}$  is the estimated triplet yield determined from the photosensitized singlet oxygen phosphorescence quantum yields. The data were obtained in aerated solutions of toluene (AuBTF complexes) and acetonitrile ( $[\text{Ru}(\text{bpy})_3]^{2+}$ ). The equation was corrected using the index of refraction values reported in the Handbook of Photochemistry. The values for  $\Delta A_{\text{x}}$  and  $\Delta A_{\text{Ru}}$  were determined from monoexponential fits of transient absorption decay traces. The weighting factor from the fits was used as the maximum  $\Delta A$  value to account for the response time of the instrument. The transient absorption traces used in the excited-state extinction coefficient determinations were all collected using laser pulse energies of  $< 200 \mu\text{J}$  in an effort to avoid the deleterious effects of nonlinear optical behavior at high laser pulse energies.<sup>20</sup> The value of  $\Delta\epsilon$  was determined at three different laser pulse energies. This multiple pulse energy treatment was completed on a second sample. The value of  $\Delta\epsilon$  given in Table 1 is the average of these 6 trials. The full  $\Delta\epsilon$  vs. wavelength spectrum for the AuBTF complexes was obtained from the  $\Delta A$  spectra of the complexes 50 ns after the laser pulse. The  $\Delta A$  spectra were normalized at the wavelength where  $\Delta\epsilon$  was determined and then multiplied by the value of  $\Delta\epsilon$  determined from the relative actinometry experiments. The data used to calculate the  $\Delta\epsilon$  values for the AuBTF complexes are shown in Figure S16.

**Delayed Fluorescence.** The delayed fluorescence behavior of the AuBTF complexes was examined at various laser pulse energies. The data were collected in freeze-pump-thaw deaerated toluene solutions. Laser pulse energies were measured using a Laser Precision Corp. RJP-735 pyroelectric energy probe and Laser Probe Inc. Rj-7620 energy ratiometer. The delayed fluorescence signal was collected using the Andor iStar ICCD camera with a gate delay of 50  $\mu\text{s}$  after the laser pulse and a gate width of 90  $\mu\text{s}$ . The fluorescence signal at each laser energy was averaged over 20 laser shots. The integrated fluorescence intensity at each laser energy was obtained by integrating the spectra from 375 – 500 nm. These integrated intensity values were normalized relative to the integrated intensity at the highest laser energy and plots of normalized, integrated fluorescence intensity vs. laser pulse energy were generated for each of the AuBTF

complexes. Double logarithm plots were also generated for these data sets. The data collected for AuBTF0 are shown in Figure 5 and the data collected for AuBTF1 and AuBTF2 are shown in Figure S14. Delayed fluorescence experiments were collected using the freeze-pump-thaw degassed samples used in the collection of the phosphorescence lifetimes.

**Triplet-Triplet Annihilation Fitting.** The delayed fluorescence experiments established the contribution of triplet-triplet annihilation to the decay of the AuBTF excited-states in toluene solution.<sup>21</sup> The triplet-triplet annihilation rate constant can be determined using equation 3.

$$(3) \quad [{}^3\text{M}^*]_t = \frac{[{}^3\text{M}^*]_0 e^{-k_T t}}{1 + [{}^3\text{M}^*]_0 (k_{\text{TT}}/k_T)(1 - e^{-k_T t})}$$

$[{}^3\text{M}^*]_t$  is the triplet excited-state concentration at some time following laser excitation,  $[{}^3\text{M}^*]_0$  is the initial excited-state concentration following laser excitation,  $k_T$  is the rate constant for the intrinsic decay of the triplet excited-state ( $\tau_T = \frac{1}{k_T}$ ), and  $k_{\text{TT}}$  is the triplet-triplet annihilation rate constant. The triplet excited-state decay traces collected in transient absorption experiments are expressed in units of  $\Delta$ absorbance vs. time. In order to fit these data, the decay traces are converted from  $\Delta$ absorbance units to concentration using the previously determined excited-state extinction coefficients. The lifetime values for the triplet excited-states were previously determined. The value of  $k_T$  from these lifetime measurements was input into the fit equation and held constant when fitting the data. Decay traces were collected at two laser pulse energies ( $\sim 1$  mJ and  $\sim 2$  mJ per pulse). The values of  $k_{\text{TT}}$  presented in Table 1 represent the average of the values obtained when fitting both decay traces. The data collected for AuBTF0 are shown in Figure 5 and the data collected for AuBTF1 and AuBTF2 are shown in Figure S15. Triplet-triplet annihilation experiments were collected using the freeze-pump-thaw degassed samples used in the collection of the phosphorescence lifetimes.

**Estimation of Singlet Excited-State Extinction Coefficient.** Our previous determinations of the quantum yield of triplet state formation and the triplet excited-state extinction coefficient allow for the estimation of the singlet excited-state extinction coefficient from the picosecond transient absorption data. This extinction coefficient can be determined using equation 4.

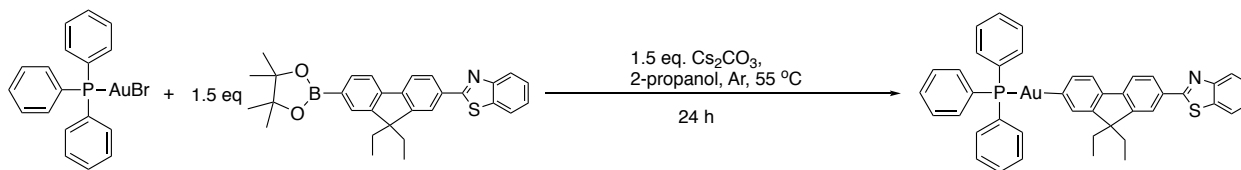
$$(4) \quad \Delta\varepsilon_{S_1-S_n} = \Delta\varepsilon_{T_1-T_n} \frac{\Delta A_{S_1-S_n} \Phi_T}{\Delta A_{T_1-T_n}}$$

$\varepsilon_{S_1-S_n}$  is the singlet excited-state extinction coefficient,  $\varepsilon_{T_1-T_n}$  is the triplet excited-state extinction coefficient,  $\Delta A_{S_1-S_n}$  is the maximum change in absorbance of the 0 ps time trace in the picosecond transient absorption data,  $\Delta A_{T_1-T_n}$  is the maximum change in absorbance of the 500 ps time trace for AuBTF0 and

AuBTF1 and the 1000 ps time trace for AuBTF2 in the picosecond transient absorption data, and  $\Phi_T$  is the quantum yield of triplet state formation.

### III. Synthesis, NMR, Mass Spectrometry and Elemental Analysis

#### AuBTF0:



To a flame-dried 25 mL round bottom flask equipped with a stir bar was added (100.05 mg, 0.186 mmol) of  $\text{Ph}_3\text{PAuBr}$ , (133.97 mg, 0.278 mmol) of pinacolboronate ester, and (181.08 mg, 0.556 mmol) of  $\text{Cs}_2\text{CO}_3$ . The flask was purged with argon for 15 min, after which 5 mL of dry 2-propanol was added via syringe. The vessel was then shielded from light and heated at 55 °C for 24 h. The contents of the flask were then cooled to room temperature yielding a bright yellow suspension that was concentrated *in vacuo*. The crude product was dissolved in 5 X 5 mL portions of benzene and filtered over Celite to yield a yellow solution which was concentrated under reduced pressure. This crude product was then subjected to vapor diffusion crystallization using dichloromethane as the solvent and pentanes as the anti-solvent (111.23 mg, 72 %).  $^1\text{H}$  NMR (500 MHz, Chloroform-*d*)  $\delta$  8.08 (d,  $J = 10.8$  Hz, 2H), 8.00 (d,  $J = 9.0$  Hz, 1H), 7.90 (d,  $J = 7.9$  Hz, 1H), 7.74 (d,  $J = 7.9$  Hz, 1H), 7.70 (d,  $J = 7.2$  Hz, 1H), 7.62 (dt,  $J = 14.7, 7.4$  Hz, 8H), 7.49 (q,  $J = 7.7$  Hz, 10H), 7.37 (t,  $J = 7.2$  Hz, 1H), 2.16 – 2.10 (m, 4H), 0.37 (t,  $J = 7.3$  Hz, 6H).  $^{31}\text{P}$  NMR (121 MHz,  $\text{CDCl}_3$ )  $\delta$  (ppm): 43.58. HRMS (FT-ICR,  $[\text{M}+\text{H}]^+$ )  $m/z$  calcd for  $\text{MH}^+ \text{C}_{42}\text{H}_{36}\text{NPSAu}^+$  814.19661, found 814.19680. Anal. Calcd for:  $\text{C}_{51}\text{H}_{56}\text{AuN}_3\text{S}$ : C, (61.99); H, (4.34); N, (1.72). Found: C, (61.83); H, (4.54); N, (1.75). Melting Point: 223 °C, decomposition 5-10 °C after melting point.

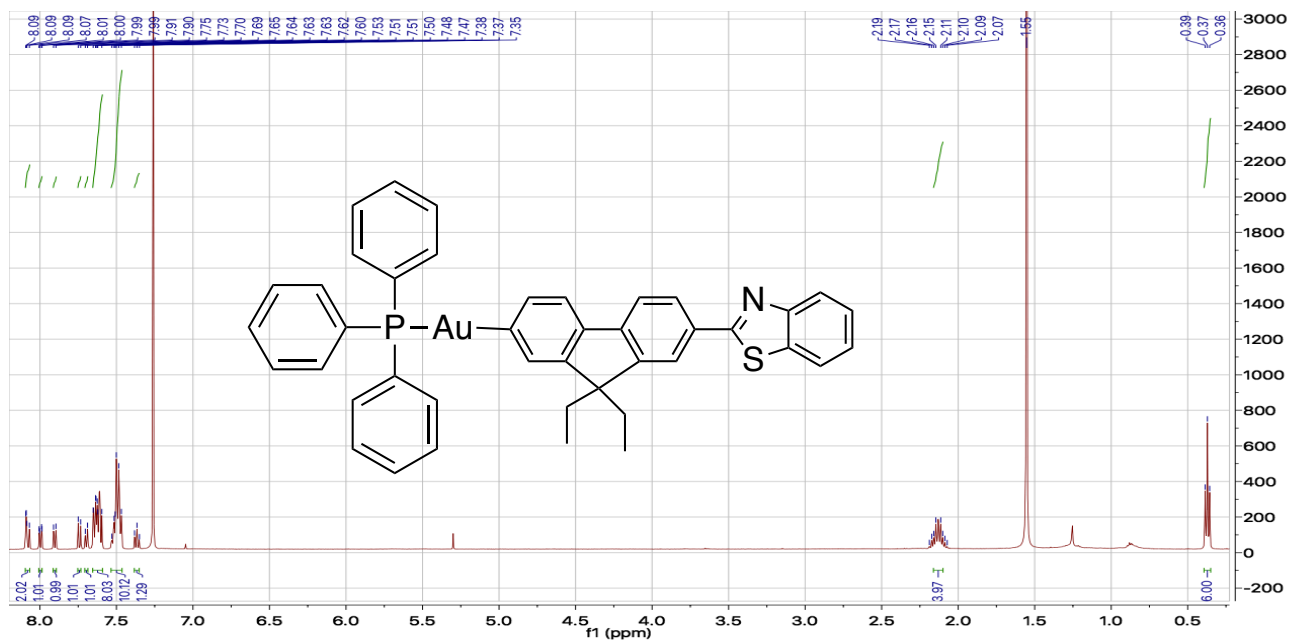


**Figure S1. <sup>1</sup>H NMR of AuBTfO**

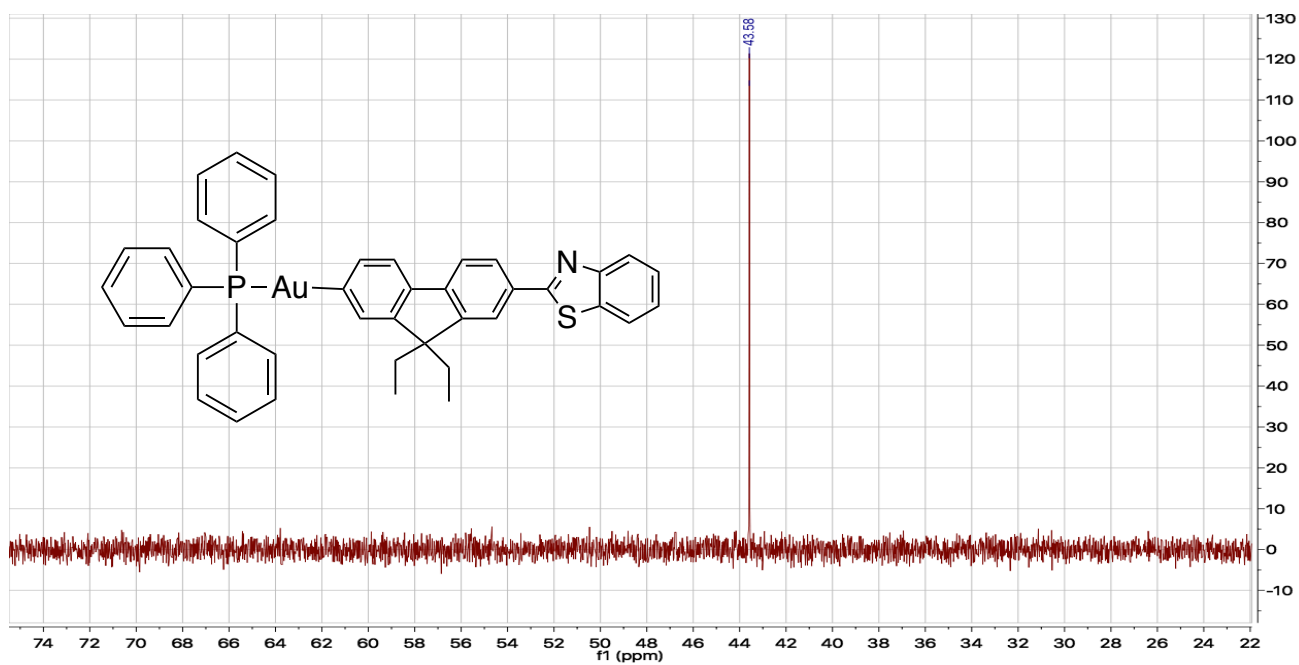


**Figure S2. <sup>31</sup>P NMR of AuBTfO**

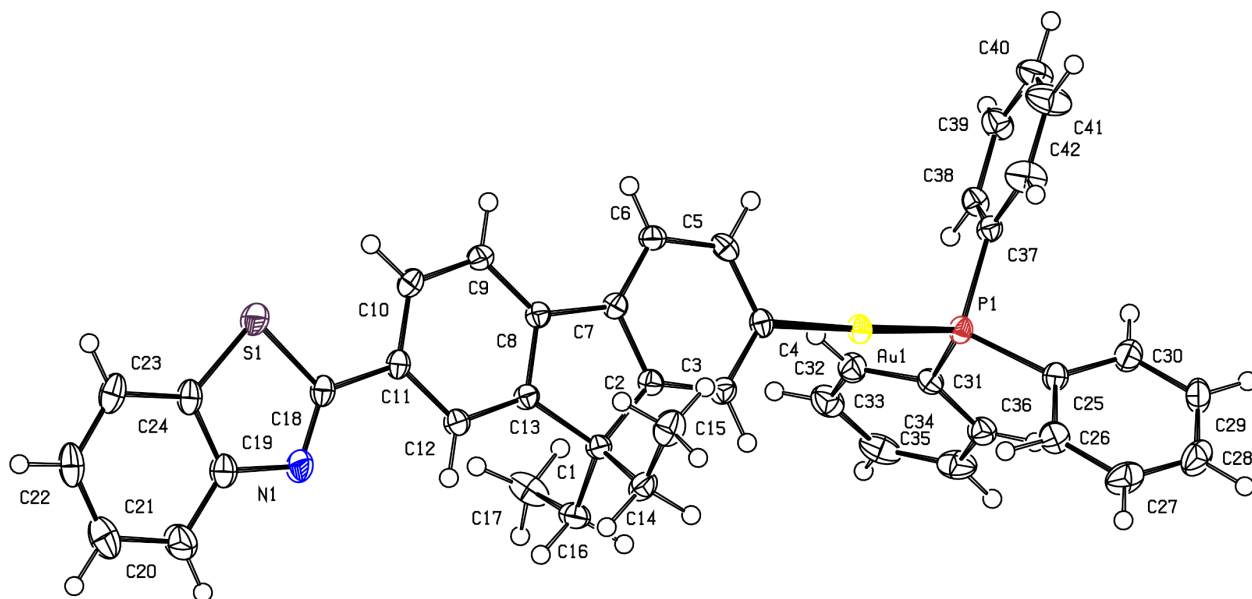
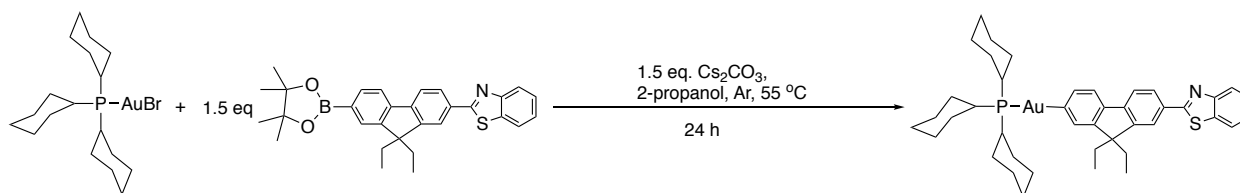


**Figure S3. Crystal Structure of AuBTF0 (50% probability level, 150 K).**

#### AuBTF1:



To a flame-dried 25 mL round bottom flask equipped with a stir bar was added 100.05 mg (0.180 mmol) of  $\text{Cy}_3\text{PAuBr}$ , 130.17 mg (0.270 mmol) of pinacolboronate ester, and 175.86 mg (0.540 mmol) of  $\text{Cs}_2\text{CO}_3$ . The flask was purged with argon for 15 min, after which 5 mL of dry 2-propanol was added via syringe. The vessel was then shielded from light and heated at 55 °C for 24 h. The contents of the flask were then cooled to room temperature yielding a bright yellow suspension that was concentrated *in vacuo*. The crude product was dissolved in  $5 \times 5$  mL portions of benzene and filtered through Celite to yield a yellow solution which was concentrated under reduced pressure. This crude product was then subjected to vapor diffusion crystallization using dichloromethane as the solvent and pentanes as the anti-solvent. (110.56 mg, 76 %).  $^1\text{H}$  NMR (500 MHz, Chloroform-*d*)  $\delta$  8.09 – 8.05 (m, 2H), 7.98 (dd,  $J = 7.8, 1.7$  Hz, 1H), 7.90 (d,  $J = 7.9$  Hz, 1H), 7.72 (d,  $J = 7.9$  Hz, 1H), 7.66 (d,  $J = 7.3$  Hz, 1H), 7.54 – 7.46 (m, 3H), 7.36 (t,  $J = 7.5$  Hz, 1H), 2.18 – 2.02 (m, 15H), 1.92 – 1.86 (m, 7H), 1.75 (d,  $J = 9.0$  Hz, 4H), 1.32 (h,  $J = 12.7, 11.2$  Hz, 11H), 0.38 (t,  $J = 7.3$  Hz, 6H).  $^{31}\text{P}$  NMR (121 MHz,  $\text{CDCl}_3$ )  $\delta$  (ppm): 57.07. HRMS (FT-ICR,  $[\text{M}+\text{H}]^+$ )  $m/z$  calcd for  $\text{MH}^+$   $\text{C}_{42}\text{H}_{54}\text{NPSAu}^+$  832.33746, found 832.33739. Anal. Calcd for:  $\text{C}_{42}\text{H}_{54}\text{AuNPS}$ : C, (60.64); H, (6.42); N, (1.68). Found: C, (60.91); H, (6.56); N, (1.75). Melting Point: 233 °C, decomposition 5-10 °C after melting point.

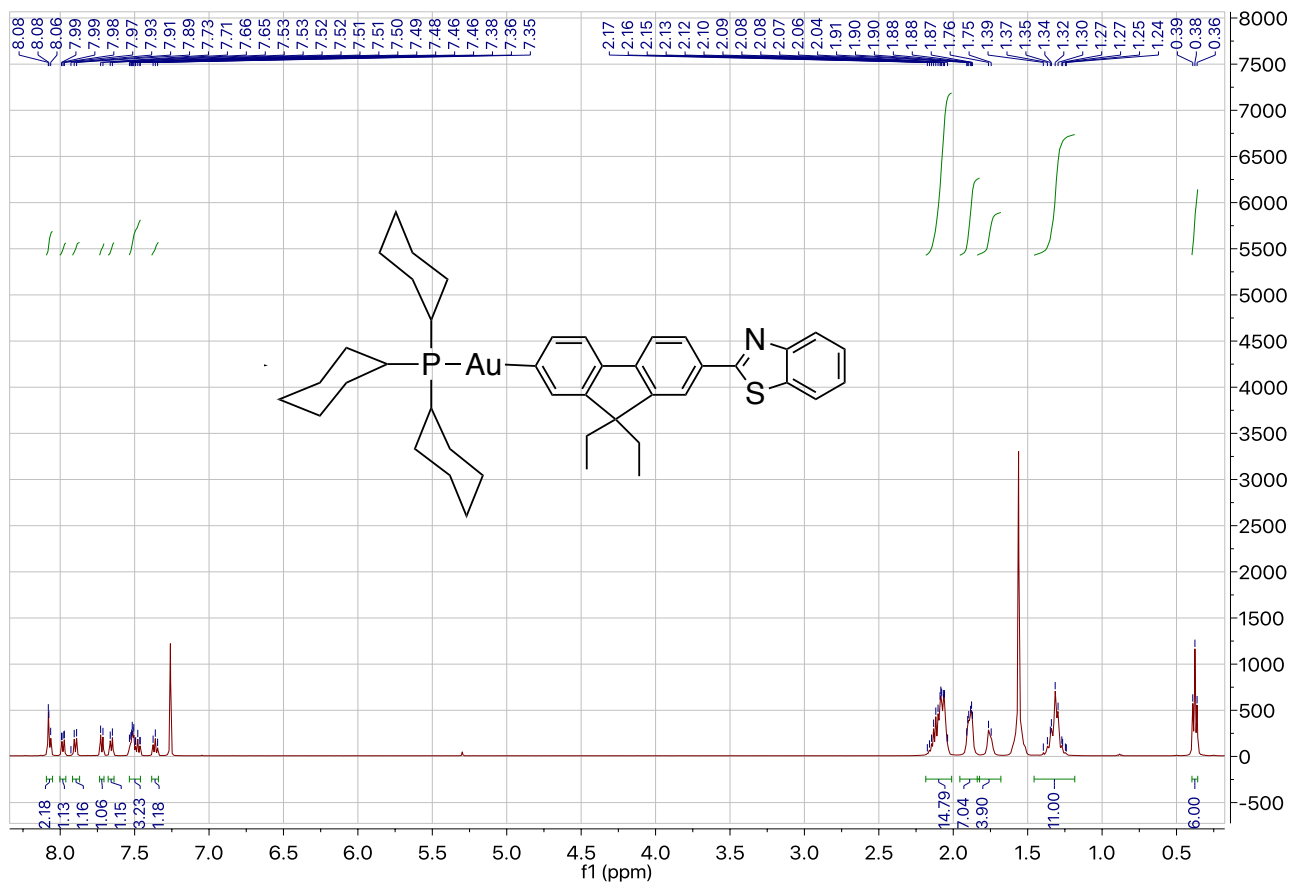
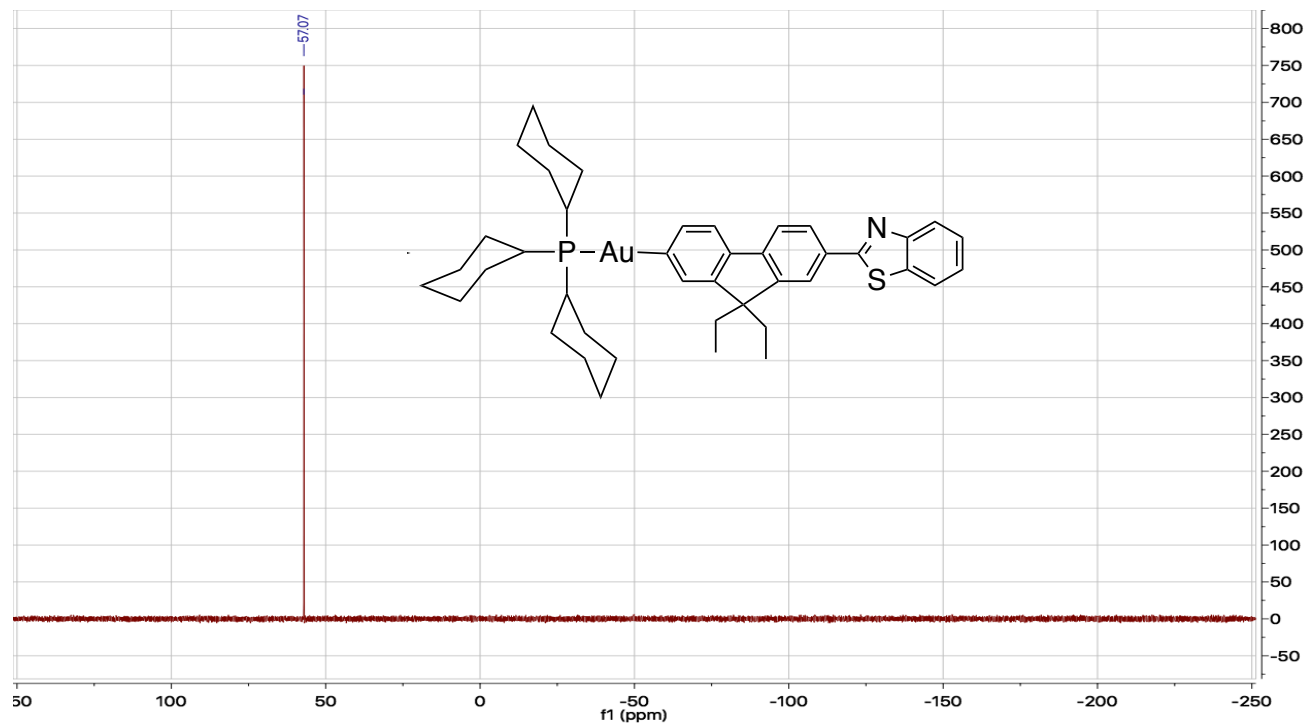
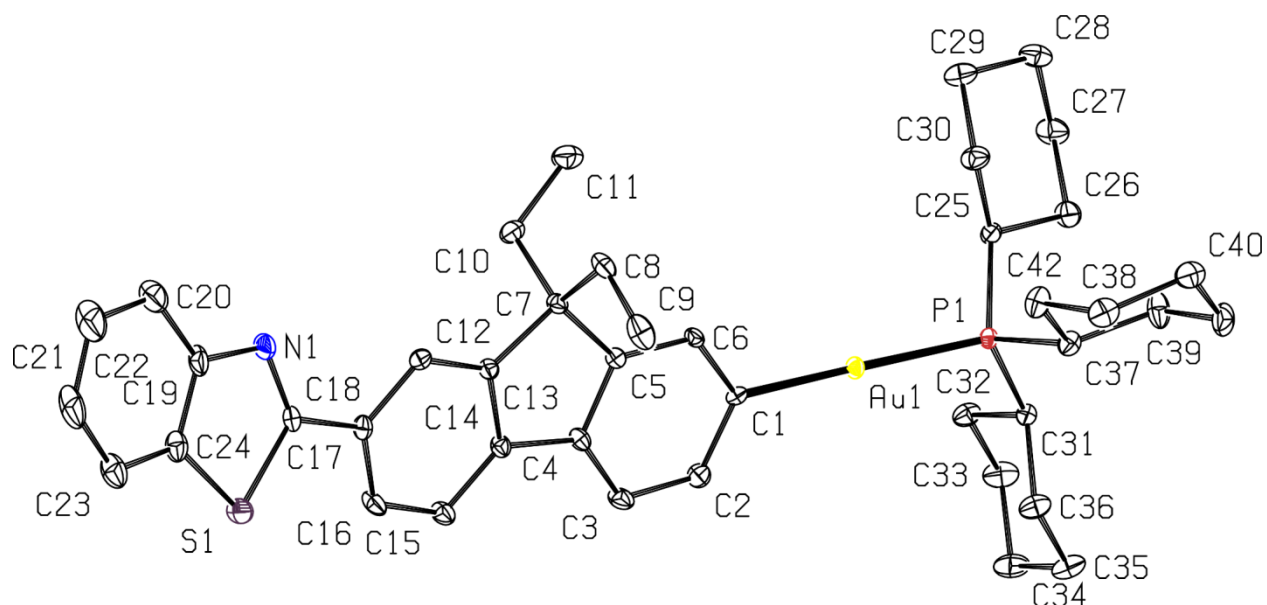


Figure S4. <sup>1</sup>H NMR of AuBTF1

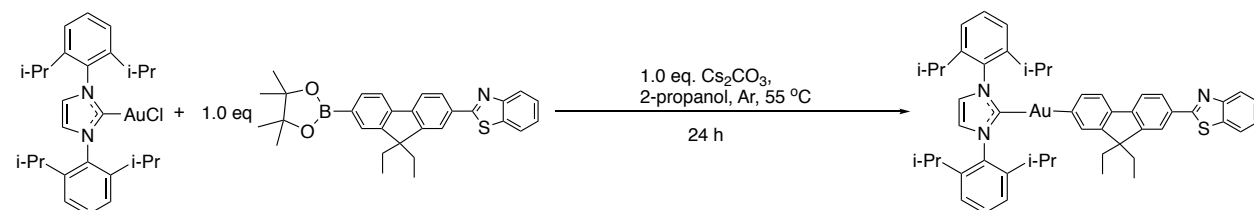


**Figure S5.**  $^{31}\text{P}$  NMR of AuBTF1



**Figure S6.** Crystal Structure of AuBTF1 (50% probability level, 100 K). Hydrogen atoms are omitted for clarity.

**AuBTF2:**



To a flame-dried 25 mL round bottom flask equipped with a stir bar was added 96.00 mg (0.155 mmol) of IPrAuCl, 74.40 mg (0.155 mmol) of pinacolboronate ester, and 100.70 mg (0.310 mmol) of  $\text{Cs}_2\text{CO}_3$ . The flask was then purged with argon for 15 min, after which 5 mL of dry 2-propanol was added via syringe. The vessel was then shielded from light and heated at 55 °C for 24 h. The contents of the flask were then allowed to cool to room temperature yielding a bright yellow suspension that was concentrated *in vacuo*. The crude product was dissolved in  $5 \times 5$  mL portions of benzene and filtered through Celite to yield a yellow solution which was subsequently concentrated under reduced pressure. This crude product was then subjected to vapor diffusion crystallization using dichloromethane as the solvent and pentanes as the anti-solvent. (77.23 mg, 53 %) Yield.  $^1\text{H}$  NMR (500 MHz, Chloroform-*d*)  $\delta$  8.04 (d,  $J = 8.2$  Hz, 1H), 8.00 (d,  $J = 1.8$  Hz, 1H), 7.95 – 7.80 (m, 2H), 7.60 (d,  $J = 7.9$  Hz, 1H), 7.47 (dt,  $J = 16.1, 8.0$  Hz, 3H), 7.40 (d,  $J = 7.4$  Hz, 1H), 7.32 (dd,  $J = 21.2, 7.6$  Hz, 5H), 7.16 (s, 2H), 7.09 (d,  $J = 7.3$  Hz, 1H), 7.03 (s, 1H), 2.71 (hept,

$J = 7.1$  Hz, 4H), 1.93 (qq,  $J = 14.1, 7.2$  Hz, 4H), 1.42 (d,  $J = 6.8$  Hz, 12H), 1.25 (d,  $J = 6.8$  Hz, 12H), 0.33 (t,  $J = 7.3$  Hz, 6H). HRMS (FT-ICR,  $[M+H]^+$ )  $m/z$  calcd for  $MH^+$   $C_{51}H_{57}N_3SAu^+$  940.39332, found 940.39341. Anal. Calcd for:  $C_{51}H_{56}AuN_3S$ : C, (65.16); H, (6.00); N, (4.47). Found: C, (65.11); H, (6.19); N, (4.44). Melting Point: 241 °C, decomposition 5-10 °C after melting point.

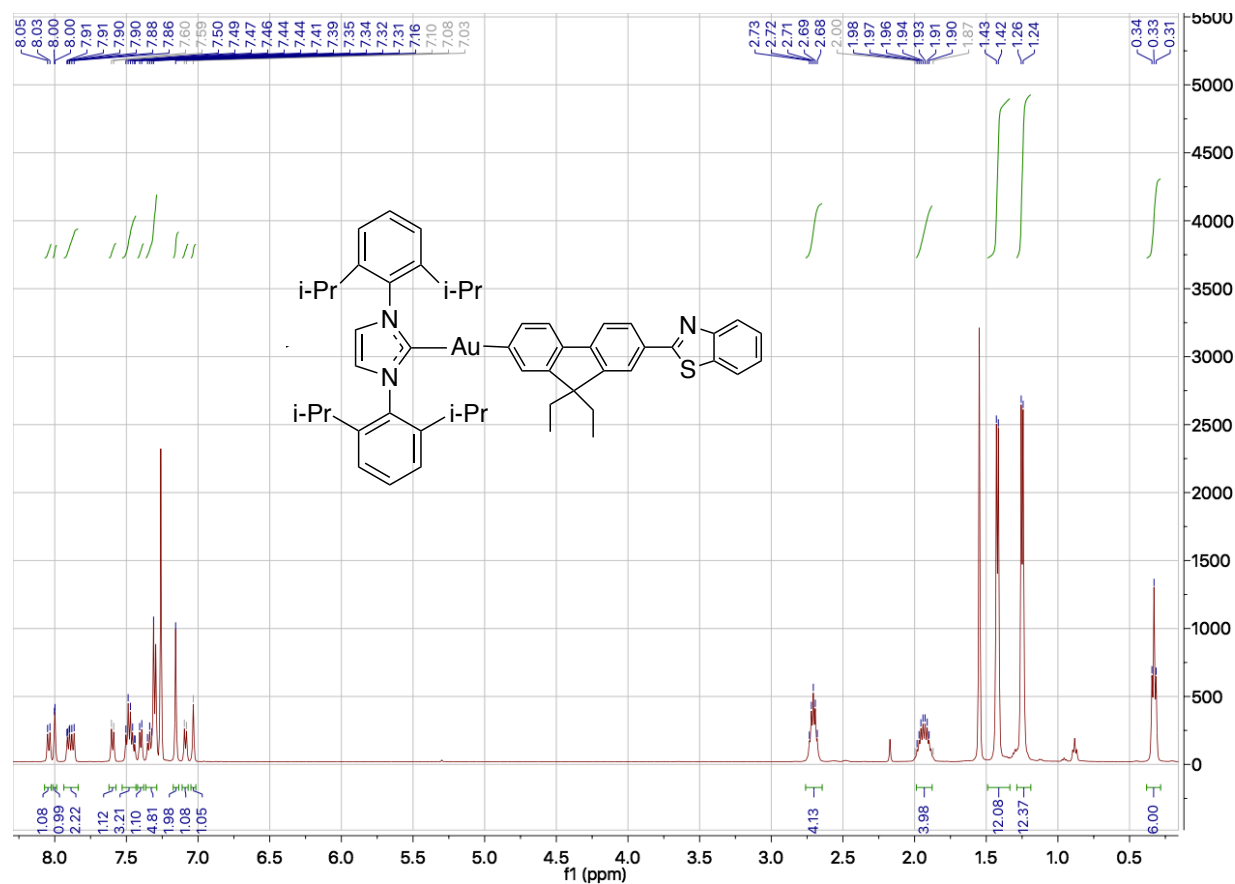
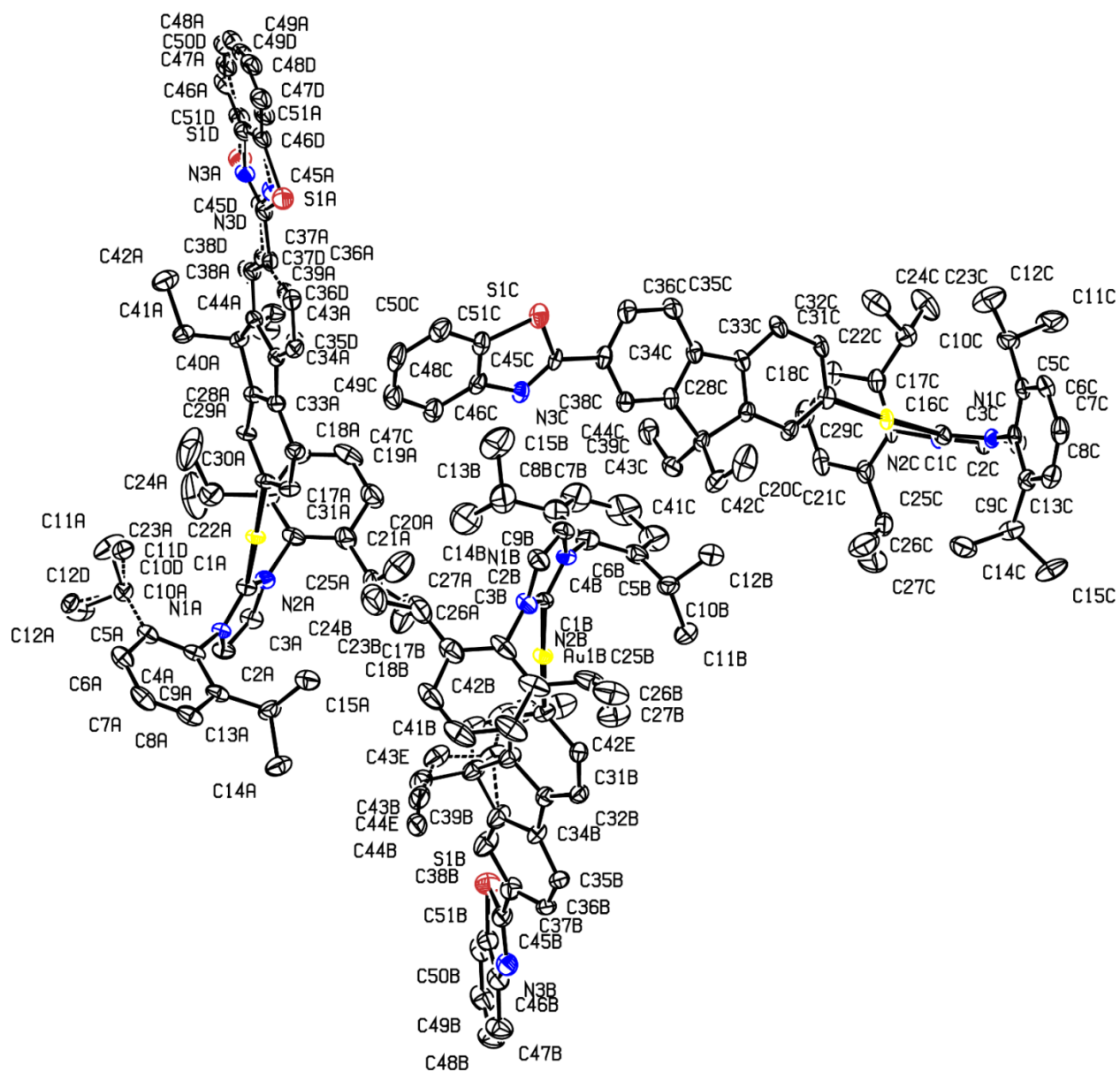
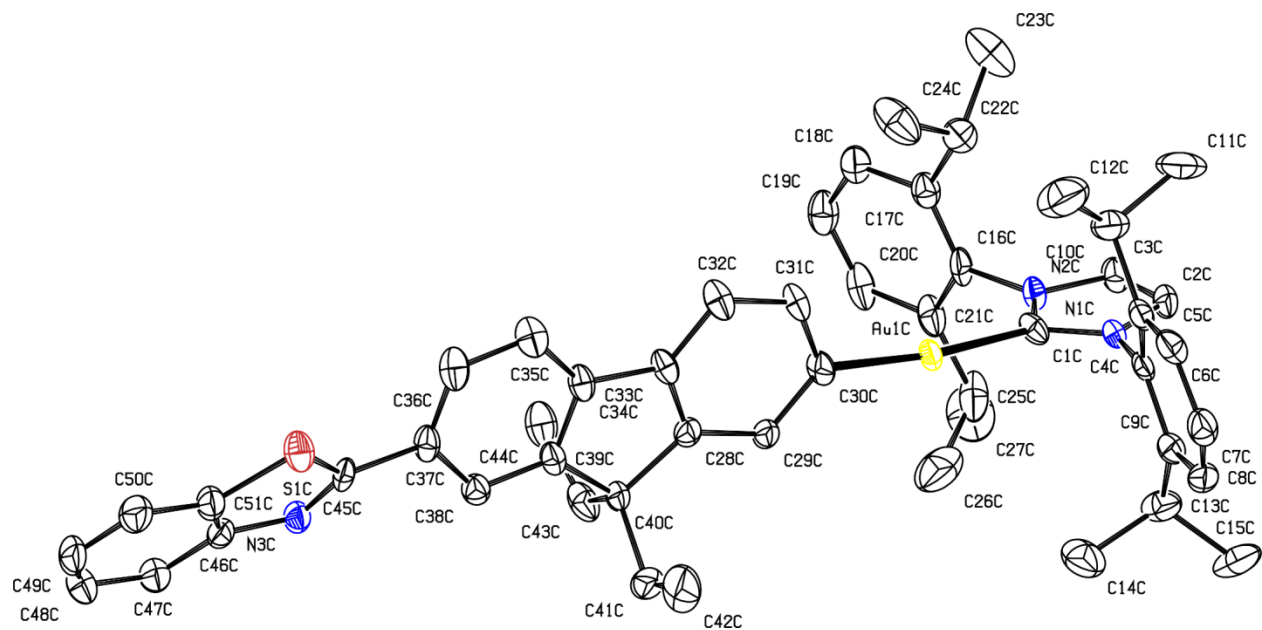


Figure S7.  $^1H$  NMR of AuBTF2



**Figure S8.** The three crystallographically independent molecules in the crystal structure of AuBTF2 (50% probability level, 100 K). Hydrogen atoms are omitted for clarity.



**Figure S9.** One of the three crystallographically independent molecules in the crystal structure of **AuBTF2** (50% probability level, 100 K). Hydrogen atoms are omitted for clarity.

## IV. Supplemental Figures

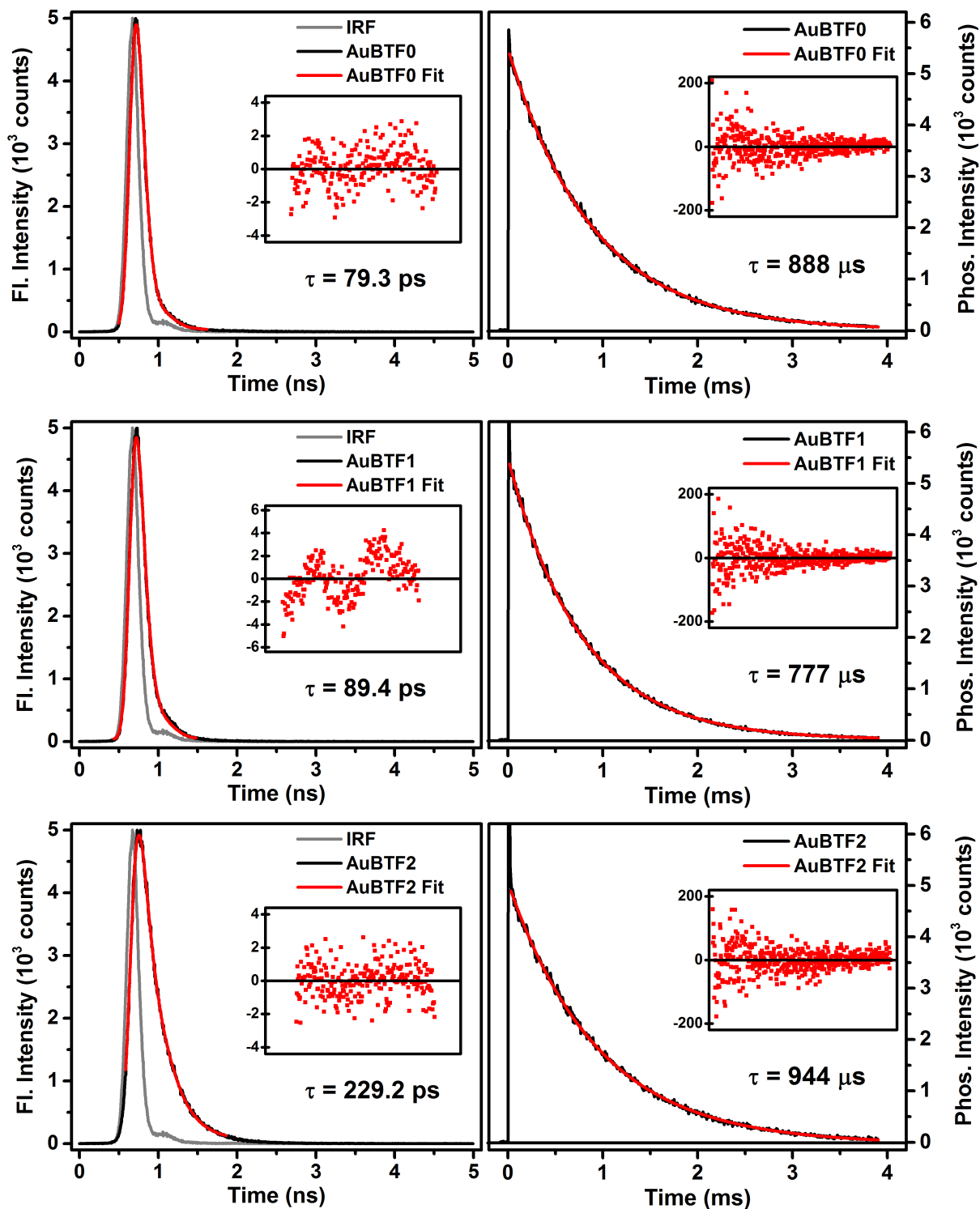


**Figure S10.** (Left) Fluorescence and (Right) phosphorescence lifetimes of (Top) AuBTF0, (Middle) AuBTF1, and (Bottom) AuBTF2 collected in toluene solution. The residuals obtained from the fits are shown in the inset. These experiments were repeated a second time. The values given in Table 1 represent the average of the two trials.

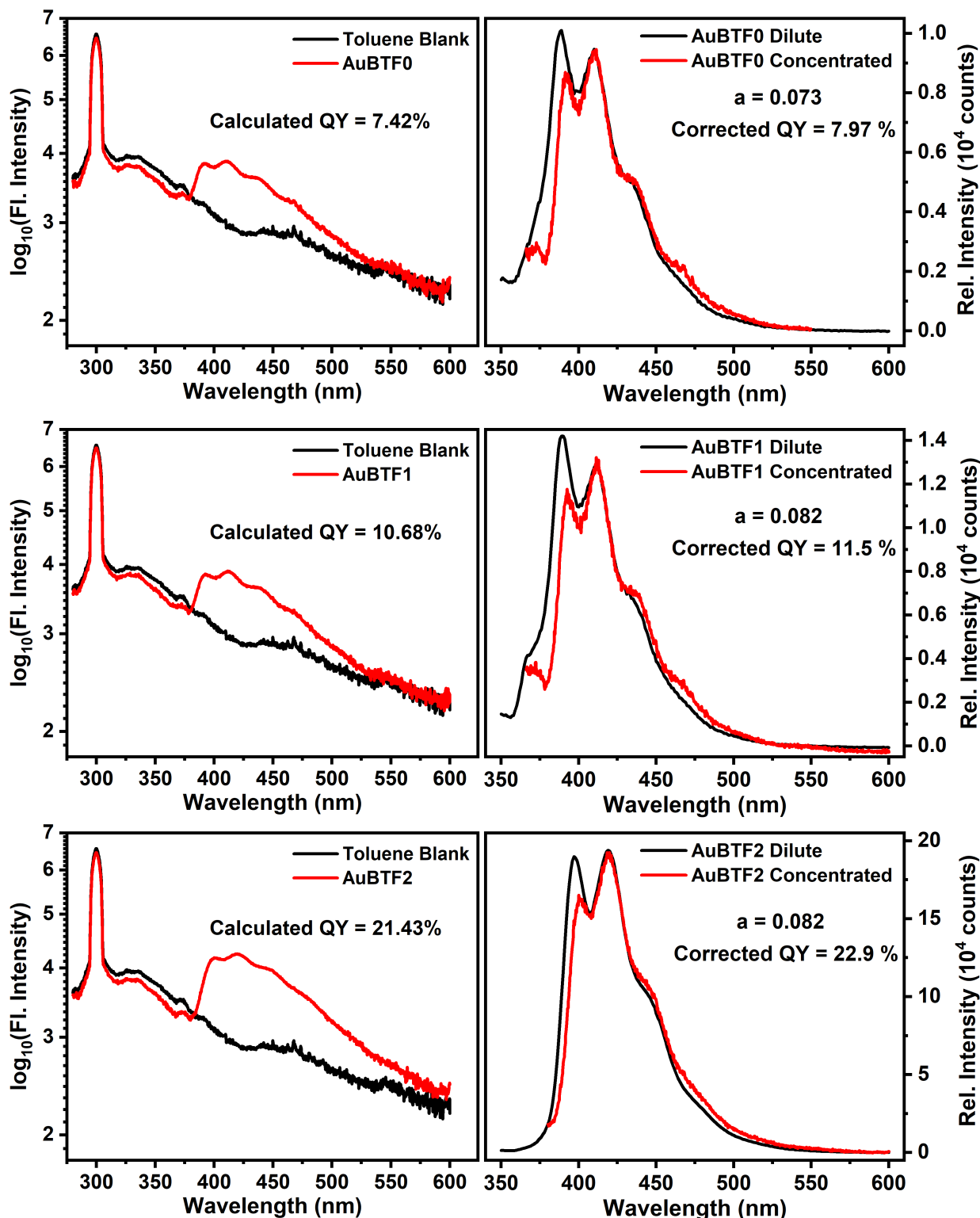


**Figure S11.** (Left) Raw and (Right) corrected fluorescence spectra in toluene solution of (Top) AuBTF0, (Middle) AuBTF1, and (Bottom) AuBTF2 used to determine fluorescence quantum yield values. The experiments were repeated a second time. The values given in Table 1 represent the average of the two trials.

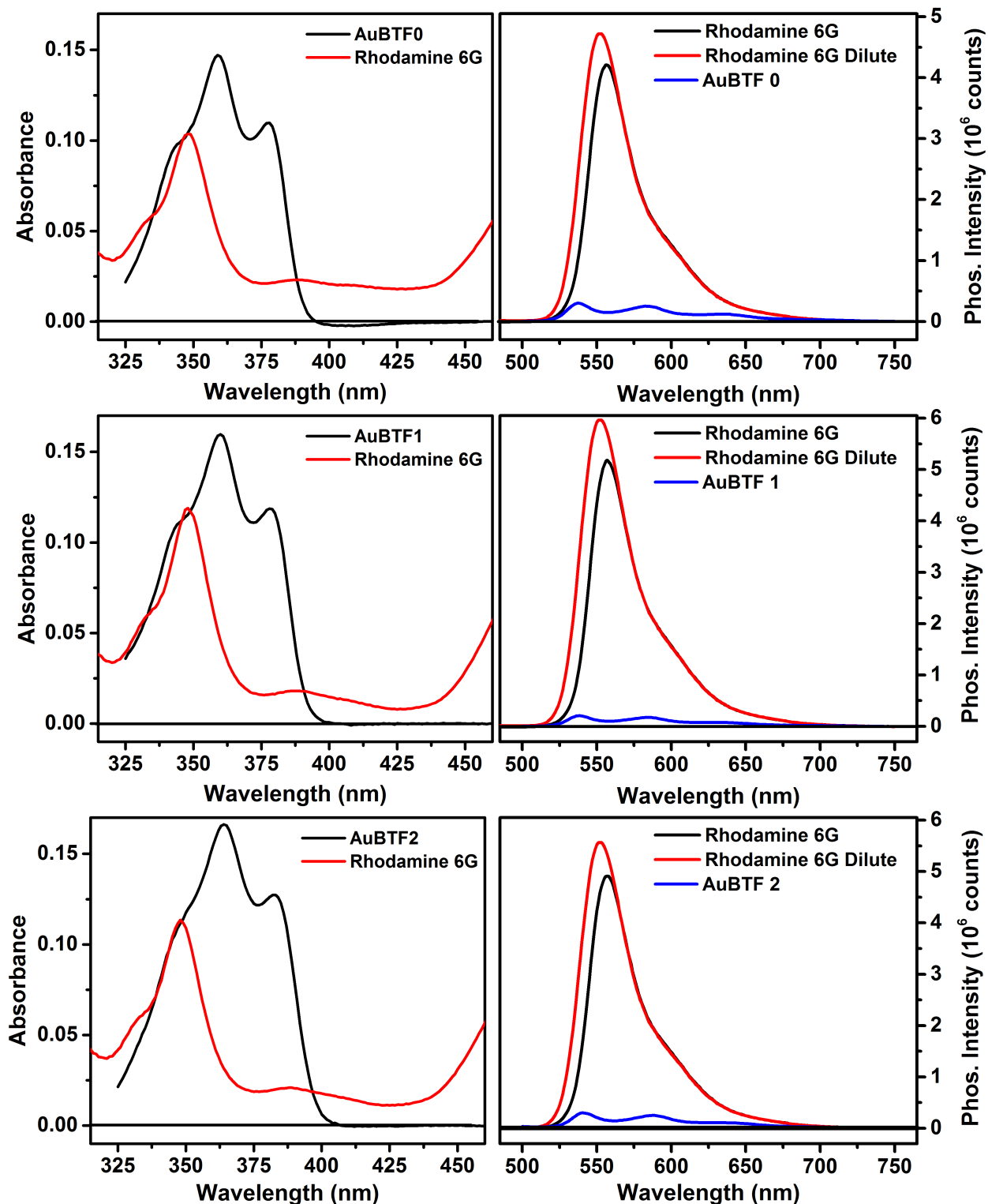


**Figure S12.** (Left) Absorption and (Right) luminescence spectra of the Rhodamine 6G reference along with (Top) AuBTF0, (Middle) AuBTF1, and (Bottom) AuBTF2 used to determine phosphorescence quantum yield values. AuBTF spectra were collected in toluene and the Rhodamine 6G spectra were collected in absolute ethanol. The experiments were repeated in duplicate for AuBTF0 and AuBTF1 and in triplicate for AuBTF2. The values given in Table 1 represent the average of these trials.

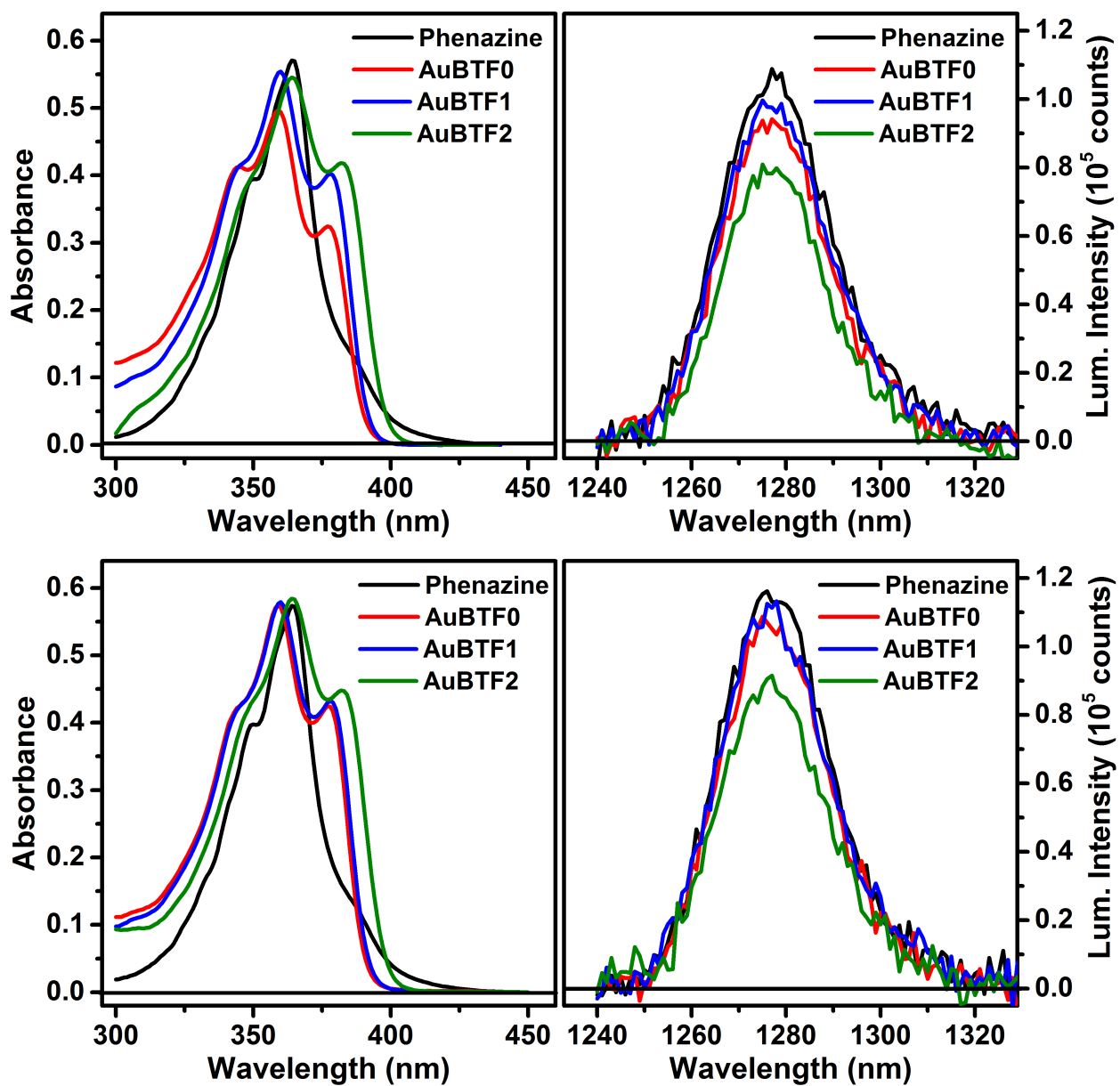


**Figure S13.** (Left) Absorption and (Right) singlet oxygen phosphorescence spectra collected from the phenazine reference and AuBTF0, AuBTF1, and AuBTF2 used to determine photosensitized singlet oxygen phosphorescence quantum yield values. All spectra were collected in benzene. Both trials of this experiment are shown above. The value reported in Table 1 represents the average value obtained from these trials.

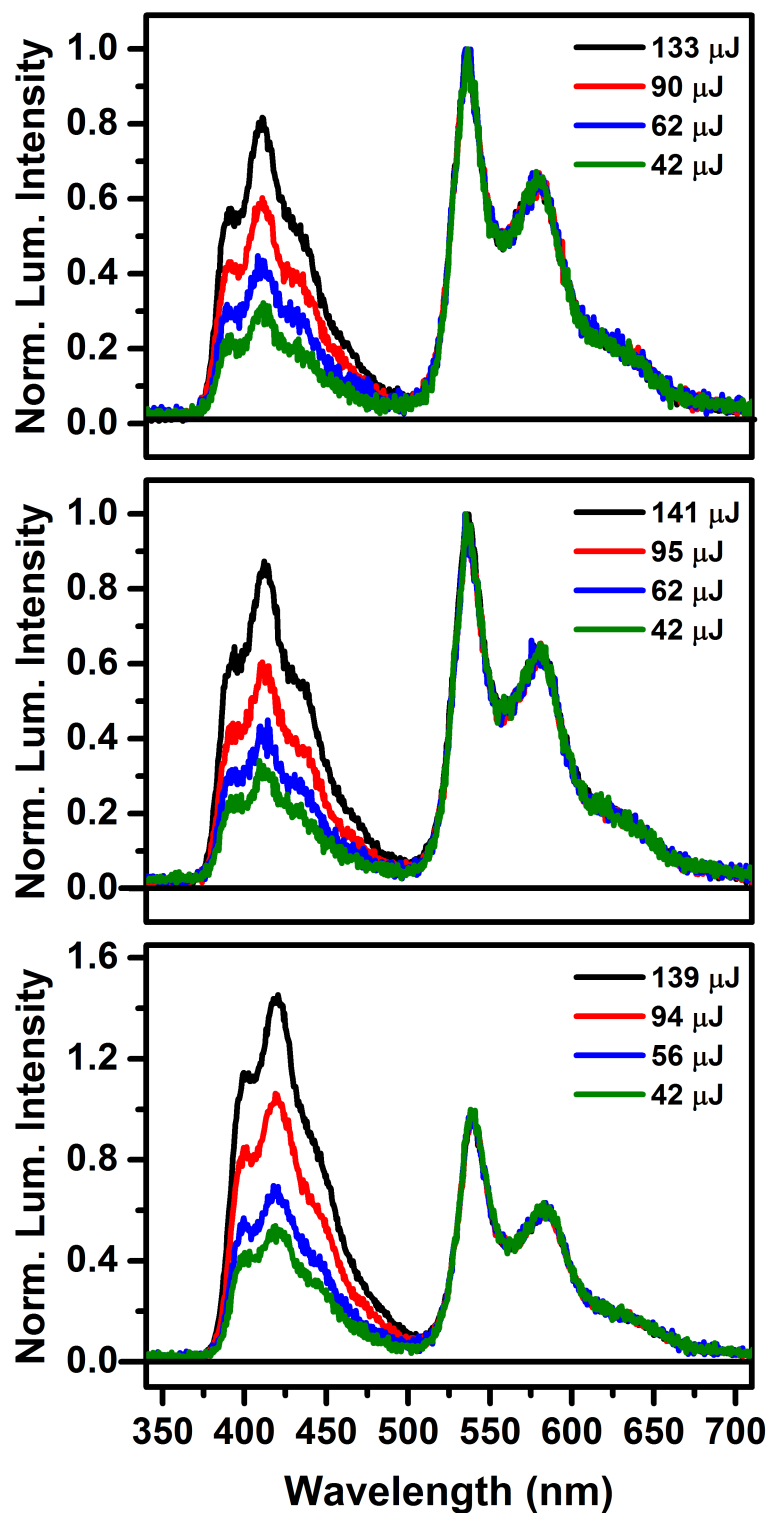


**Figure S14.** Delayed fluorescence observed in samples of (Top) AuBTF0, (Middle) AuBTF1, and (Bottom) AuBTF2. The data were collected in freeze-pump-thaw degassed toluene solution. The spectra were collected on the Andor iStar ICCD camera with a gate delay of 50  $\mu\text{s}$  and a gate width of 90  $\mu\text{s}$ . The signal is normalized to the phosphorescence maximum to demonstrate the influence of laser pulse energy on the magnitude of the delayed fluorescence signal.

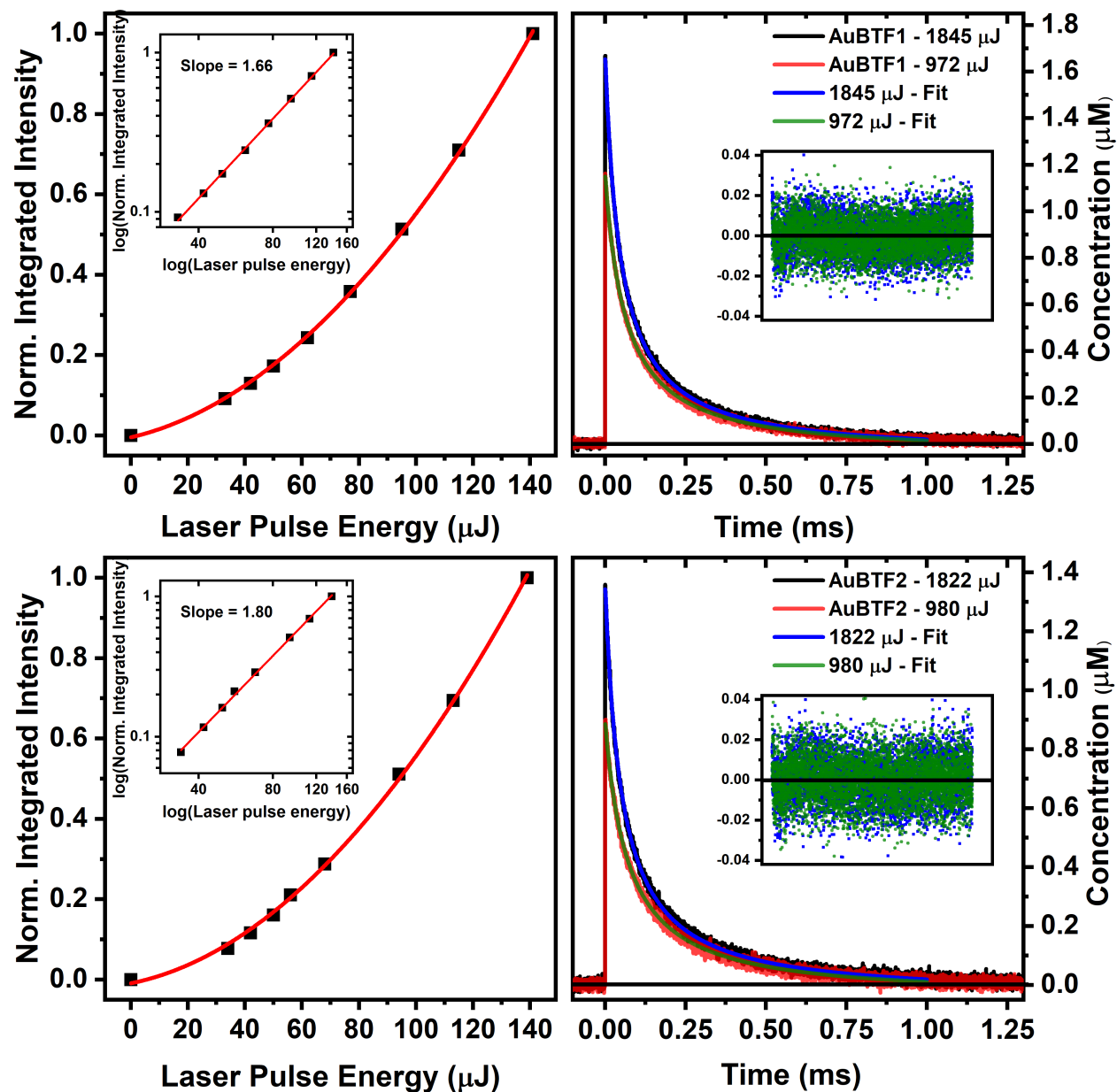


**Figure S15.** (Left) Fits of the normalized, integrated fluorescence intensity vs. laser pulse energy and (Right) triplet-triplet annihilation fitting of excited-state decay traces in freeze-pump-thaw deaerated toluene solution of (Top) AuBTF1 and (Bottom) AuBTF2. The insets represent the double logarithm plot (Left) and residuals of the data fit (Right).

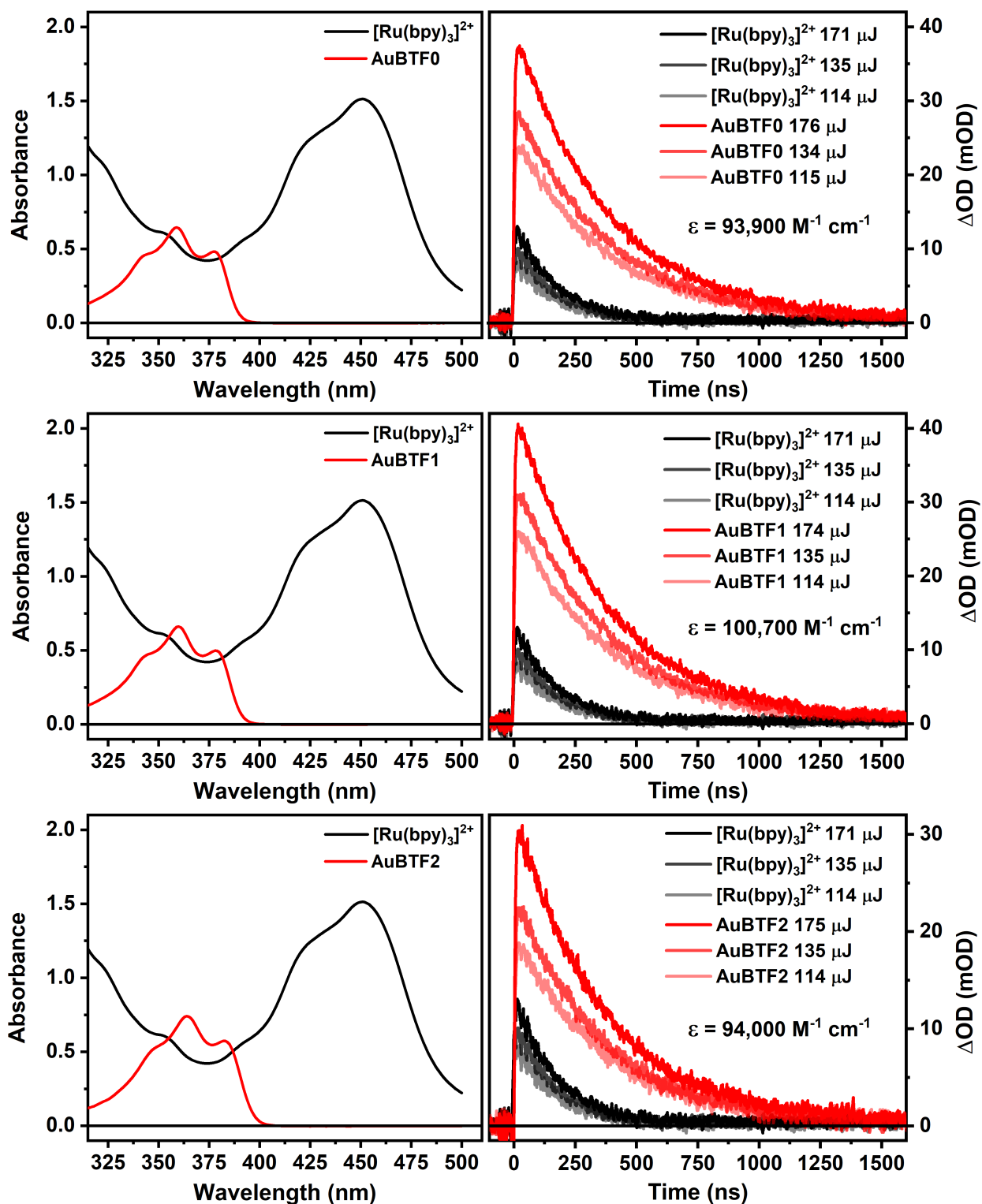


**Figure S16.** (Right) Absorbance and (Left) excited-state absorption decay traces at three laser excitation energies in samples of (Top) AuBTF0 (547 nm), (Middle) AuBTF1 (550 nm), and (Bottom) AuBTF2 (562 nm) along with [Ru(bpy)<sub>3</sub>]<sup>2+</sup> (370 nm). The AuBTF data was collected in aerated toluene solution and the [Ru(bpy)<sub>3</sub>]<sup>2+</sup> was collected in aerated acetonitrile solution. All samples were excited at 355 nm.

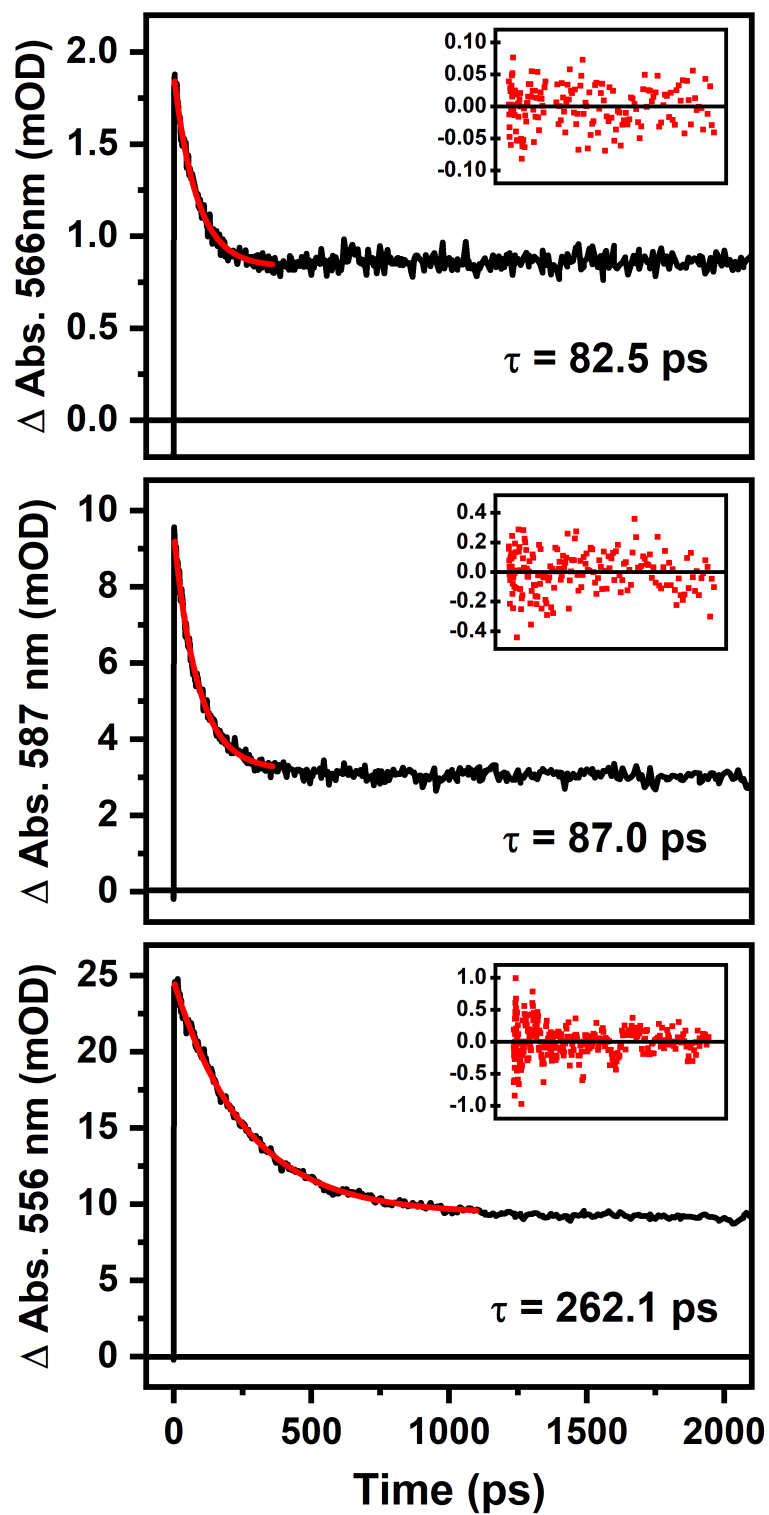


**Figure S17.** Ultrafast transient absorption decay trace collected at a single wavelength for (Top) AuBTF0, (Middle) AuBTF1, and (Bottom) AuBTF2 in aerated toluene solution. The residual values obtained from monoexponential decay fits of the data are shown in the inset. The lifetime value represented in Table 1 is the average of the lifetime value obtained at 10 unique wavelengths in transient absorption spectrum.

**Calculations.** Spin-restricted and time-dependent density-functional theory computations proceeded in Gaussian16 rev. A.03.<sup>2</sup> Geometries were optimized with the 6-31G(d) basis set for nonmetal atoms and the Stuttgart-Dresden effective core potential and basis set for Au.<sup>3</sup> Optimizations proceeded without constraints, and harmonic frequency calculations found all real vibrational frequencies, confirming that converged structures are local energy minima. Final single-point calculations employed the exchange and correlation functionals of Perdew, Burke, and Ernzerhof (PBE0),<sup>4</sup> and the TZVP basis set of Godbelt, Andzelm, and co-workers for nonmetals.<sup>5</sup> For metal atoms, the Stuttgart-Dresden effective core potential and basis set were used; scalar relativistic effects are included implicitly. Continuum solvation in toluene was imposed using the integral equation formalism of the polarizable continuum model.<sup>6-9</sup> Population analyses were performed with the AOMix-CDA program of Gorelsky.<sup>10,11</sup>

**Table 1. AuBTF1:** Summary of calculated electronic transitions to Franck-Condon singlet states. MO 181: HOMO; MO 182: LUMO.

#	nm	1000 cm <sup>-1</sup>	eV	<i>f</i>	Assignment
1	372.9	26.82	3.325	1.6354	181→182(98.3%) (HOMO→LUMO)
2	303.6	32.94	4.084	0.0030	180→182(94.2%)
3	292.5	34.19	4.239	0.0149	178→182(45.3%) 181→183(18.2%) 177→182(11.5%)
4	291.8	34.26	4.248	0.0123	179→182(82.2%)
5	285.2	35.07	4.348	0.0421	181→183(24.5%) 176→182(23.4%) 177→182(16.6%) 178→182(13.1%)
6	279.0	35.84	4.443	0.0931	177→182(63.0%) 178→182(29.7%)
7	264.4	37.83	4.690	0.1960	181→183(41.5%) 181→184(20.5%) 181→185(15.7%) 176→182(12.1%)
8	259.7	38.50	4.774	0.0210	181→184(49.2%) 176→182(31.3%)
9	257.0	38.91	4.825	0.0021	181→186(64.4%) 181→185(30.0%)
10	253.7	39.41	4.886	0.0008	173→182(92.5%)
11	253.6	39.43	4.889	0.0258	181→185(36.1%) 181→186(20.0%) 181→184(13.4%) 176→182(12.5%)
12	245.0	40.81	5.060	0.0064	175→182(94.7%)
13	241.9	41.35	5.126	0.0184	180→183(53.0%) 180→185(18.5%)
14	240.6	41.56	5.153	0.0024	181→187(60.1%) 180→183(11.8%)
15	240.6	41.57	5.154	0.0102	180→186(35.1%) 181→187(27.7%) 180→185(12.2%)
16	238.2	41.97	5.204	0.0060	180→185(31.1%) 180→189(19.8%) 180→184(19.5%) 180→186(16.4%)
17	237.2	42.16	5.227	0.0560	181→189(37.5%) 179→183(17.0%) 180→186(16.4%)
18	235.5	42.46	5.264	0.0258	181→188(80.2%)

19	233.5	42.83	5.311	0.0001	181→190(88.2%) 177→190(10.3%)
20	227.7	43.93	5.446	0.1100	174→182(32.8%) 178→184(15.7%)
21	224.7	44.51	5.518	0.0164	179→183(54.9%)
22	222.9	44.86	5.562	0.0482	178→183(32.9%) 174→182(32.3%) 177→184(15.0%)
23	221.6	45.13	5.595	0.0022	177→183(24.4%) 178→183(12.7%) 178→184(10.9%) 180→187(10.6%)
24	218.7	45.73	5.670	0.0816	180→187(67.7%) 177→183(13.0%)
25	217.6	45.95	5.697	0.0038	179→186(51.1%) 179→185(36.7%)
26	217.1	46.06	5.710	0.0477	178→184(27.1%) 177→183(22.9%)
27	216.3	46.23	5.731	0.0001	172→182(61.8%) 168→182(27.8%)
28	215.3	46.44	5.758	0.0329	180→188(50.6%) 180→189(16.8%)
29	214.7	46.57	5.774	0.4645	177→184(41.9%) 178→183(23.4%)
30	214.3	46.65	5.785	0.1260	179→184(17.0%) 177→183(16.0%) 181→189(13.9%) 179→186(11.2%)
31	214.2	46.68	5.787	0.0014	180→184(62.1%) 180→189(18.4%)
32	213.2	46.90	5.814	0.0365	170→182(55.4%) 171→182(16.0%)
33	212.6	47.04	5.833	0.0010	178→190(73.4%) 177→190(16.9%)
34	212.5	47.05	5.834	0.0093	169→182(72.6%)
35	211.5	47.28	5.862	0.0073	181→191(49.8%) 178→184(11.9%)
36	208.7	47.92	5.941	0.1667	176→183(35.8%) 178→185(21.9%)
37	208.0	48.08	5.961	0.0051	180→189(34.6%) 180→185(20.8%) 180→188(12.3%)
38	207.6	48.16	5.971	0.0018	181→192(68.3%)
39	207.3	48.23	5.980	0.0384	175→186(32.1%) 175→185(27.2%)
40	207.0	48.31	5.989	0.0004	167→182(36.9%) 168→182(20.6%) 164→182(15.9%)

**Table 2. AuBTF1:** Summary of calculated electronic transitions to Franck-Condon triplet states. MO 181: HOMO; MO 182: LUMO.

#	nm	1000 cm <sup>-1</sup>	eV	Assignment
1	526.5	18.99	2.355	181→182(81.6%) (HOMO→LUMO)
2	394.6	25.34	3.142	178→182(35.4%) 181→183(15.0%) 177→182(13.1%)
3	346.2	28.88	3.581	177→182(28.3%) 178→182(19.9%)
4	327.0	30.59	3.792	176→182(16.6%) 179→182(14.5%) 178→182(13.5%)
5	322.1	31.04	3.849	179→182(40.5%) 181→183(12.4%) 176→182(10.9%)
6	318.3	31.42	3.895	180→182(81.7%)
7	317.6	31.48	3.903	No transition contributes more than 10%.
8	316.0	31.65	3.924	176→182(32.0%) 177→182(16.4%) 179→182(12.5%)
9	304.2	32.87	4.076	178→184(13.7%) 177→184(12.5%) 176→183(10.6%)

10	298.5	33.50	4.153	176→182(29.3%) 181→183(20.0%) 177→182(16.0%)
11	287.1	34.84	4.319	181→184(32.9%) 178→184(18.9%) 181→185(11.7%)
12	280.3	35.68	4.424	181→189(20.6%) 174→182(12.0%) 179→189(10.9%)
13	278.8	35.86	4.446	173→182(86.2%)
14	276.7	36.14	4.480	181→189(31.4%) 179→189(12.2%)
15	268.4	37.26	4.620	181→189(20.0%)
16	264.2	37.84	4.692	180→186(49.4%) 180→185(30.7%)
17	259.9	38.48	4.771	180→183(22.1%) 180→186(13.1%) 180→188(10.9%) 175→182(10.5%) 180→184(10.2%) 180→182(10.1%)
18	257.9	38.77	4.807	181→186(62.9%) 181→185(30.2%)

**Optimized Cartesian Coordinates (Å)**  
**Au-BTF0**

81

P	3.418635	-1.374176	-0.099802
C	1.891369	-1.474997	-1.097266
C	1.119911	-0.314175	-1.237322
C	1.469241	-2.660170	-1.708202
C	-0.064531	-0.344323	-1.966271
H	1.453252	0.614357	-0.778955
C	0.285587	-2.683767	-2.442559
H	2.067195	-3.562817	-1.617071
C	-0.482364	-1.528981	-2.570257
H	-0.656348	0.560684	-2.070845
H	-0.034101	-3.606997	-2.917909
H	-1.403362	-1.549778	-3.146314
C	4.400529	-2.840762	-0.570972
C	4.276189	-4.069751	0.085810
C	5.297816	-2.717434	-1.639415
C	5.033548	-5.162609	-0.328966
H	3.594389	-4.171994	0.925731
C	6.047954	-3.813687	-2.053749
H	5.412482	-1.758359	-2.139741
C	5.916824	-5.036734	-1.398777
H	4.934960	-6.112985	0.188323
H	6.742789	-3.708856	-2.882239
H	6.508909	-5.890147	-1.717641
C	2.884977	-1.682713	1.619783
C	1.698368	-2.357911	1.925711
C	3.709455	-1.231786	2.658083
C	1.348456	-2.587231	3.254171
H	1.043705	-2.697297	1.127447
C	3.358260	-1.467984	3.983604
H	4.621605	-0.687012	2.424762

C	2.177778	-2.145509	4.282635
H	0.423654	-3.108833	3.484814
H	4.002159	-1.112623	4.783149
H	1.900148	-2.322262	5.318115
Au	4.578690	0.645452	-0.380384
C	5.595077	2.400597	-0.629550
C	6.962056	2.509552	-0.292718
C	4.963782	3.550849	-1.147370
C	7.680578	3.692194	-0.455297
H	7.481920	1.642236	0.108926
C	5.666991	4.736440	-1.315527
H	3.910347	3.511247	-1.420984
C	7.026420	4.810217	-0.969796
H	8.733571	3.736328	-0.183941
C	5.168390	6.067955	-1.854300
C	7.501330	6.161742	-1.249475
C	6.428221	6.913206	-1.768066
C	8.755701	6.748421	-1.086184
C	6.603157	8.237006	-2.120755
C	8.929220	8.080477	-1.441485
H	9.591389	6.179550	-0.687361
C	7.866388	8.836737	-1.958702
H	5.791064	8.836448	-2.522736
H	9.908244	8.536481	-1.313567
C	4.030000	6.650407	-0.985997
H	3.160291	5.986457	-1.086003
H	3.731165	7.614196	-1.421175
C	4.661791	5.945907	-3.309582
H	3.761031	5.316856	-3.298288
H	4.335648	6.942119	-3.639344
C	5.665671	5.379912	-4.305491
H	5.223882	5.327705	-5.306663
H	6.562496	6.005775	-4.367871
H	5.978883	4.369097	-4.022769
C	4.362596	6.835559	0.488823
H	5.203698	7.523901	0.625158
H	3.501990	7.248407	1.026567
H	4.627612	5.882468	0.959080
C	8.031000	10.238348	-2.337447
N	7.077384	10.974368	-2.822407
S	9.590659	11.062301	-2.157361
C	7.509118	12.251789	-3.090120
C	8.867196	12.507634	-2.793801
C	6.716023	13.278291	-3.619034
C	9.440406	13.758697	-3.014548
C	7.285330	14.522766	-3.838982
H	5.672941	13.080652	-3.846306
C	8.635061	14.761770	-3.539774
H	10.484609	13.946734	-2.784000
H	6.679103	15.325643	-4.248848
H	9.059495	15.745274	-3.720545

## Au-BTF1

99

P	3.200936	-1.676677	-0.142914
C	1.491800	-1.737413	-0.891077
C	0.600967	-2.927745	-0.508780
C	0.731906	-0.417504	-0.679560
H	1.713331	-1.812345	-1.969363
C	-0.702256	-2.912835	-1.311164
H	0.356286	-2.865773	0.560224
H	1.121911	-3.879025	-0.659233
C	-0.578122	-0.404551	-1.467714
H	0.516583	-0.286135	0.390299
H	1.362141	0.429997	-0.974422
C	-1.459845	-1.601530	-1.120816
H	-1.326858	-3.764367	-1.013843
H	-0.471011	-3.050410	-2.377881
H	-1.112661	0.534238	-1.278008
H	-0.348511	-0.422689	-2.543551
H	-2.370544	-1.595059	-1.732172
H	-1.784129	-1.521214	-0.072769
C	4.267456	-2.750960	-1.231034
C	5.659833	-2.930045	-0.608070
C	3.698018	-4.087946	-1.722342
H	4.393781	-2.108403	-2.117712
C	6.616029	-3.614740	-1.584951
H	5.581461	-3.541956	0.301955
H	6.062342	-1.954896	-0.303790
C	4.670121	-4.761770	-2.694557
H	3.514321	-4.759859	-0.874158
H	2.734046	-3.934803	-2.221293
C	6.052987	-4.946623	-2.074842
H	7.591087	-3.762128	-1.104770
H	6.786204	-2.951578	-2.445471
H	4.259452	-5.727379	-3.014636
H	4.758660	-4.142778	-3.599476
H	6.735796	-5.405553	-2.800259
H	5.980290	-5.644003	-1.226986
C	3.235239	-2.341265	1.597310
C	2.351425	-1.478573	2.513335
C	2.982086	-3.835666	1.836502
H	4.280204	-2.136699	1.882620
C	2.558875	-1.846049	3.982507
H	1.294329	-1.629399	2.252817
H	2.569831	-0.414901	2.353768
C	3.192373	-4.187180	3.311852
H	1.957398	-4.096807	1.547268
H	3.651146	-4.444200	1.219020
C	2.317691	-3.333691	4.226551
H	1.895282	-1.240100	4.611477

H	3.588136	-1.590585	4.274081
H	2.986050	-5.253311	3.467968
H	4.249745	-4.030977	3.571892
H	2.508893	-3.583815	5.277275
H	1.259298	-3.565611	4.035839
Au	4.121895	0.497683	-0.131635
C	4.968448	2.362101	-0.118055
C	5.696412	2.828684	0.999186
C	4.850330	3.238318	-1.217818
C	6.280731	4.092872	1.040372
H	5.810173	2.181667	1.866821
C	5.427119	4.501511	-1.192765
H	4.298068	2.921912	-2.101930
C	6.143371	4.932262	-0.063868
H	6.833326	4.414359	1.921228
C	5.408677	5.575887	-2.268783
C	6.631333	6.284598	-0.314457
C	6.211096	6.679643	-1.600139
C	7.385495	7.151990	0.475091
C	6.538978	7.926857	-2.094214
C	7.714083	8.406353	-0.024198
H	7.715857	6.859336	1.468226
C	7.299919	8.808547	-1.303195
H	6.226372	8.253210	-3.082161
H	8.302135	9.081494	0.593222
C	3.970338	6.035300	-2.598923
H	3.448735	5.189388	-3.067544
H	4.032383	6.819850	-3.365895
C	6.080934	5.093722	-3.574462
H	5.457987	4.292109	-3.994652
H	6.046941	5.919768	-4.298436
C	7.514477	4.600516	-3.427237
H	7.910150	4.277985	-4.396643
H	8.170694	5.389388	-3.043903
H	7.572943	3.749851	-2.739710
C	3.158130	6.540774	-1.413748
H	3.633647	7.409141	-0.945046
H	2.155653	6.842284	-1.736941
H	3.046221	5.764277	-0.649405
C	7.635728	10.123894	-1.843301
N	7.272549	10.539061	-3.018962
S	8.592112	11.285800	-0.905149
C	7.724258	11.813155	-3.268758
C	8.474303	12.405911	-2.227720
C	7.495484	12.534514	-4.447626
C	8.994192	13.693835	-2.343385
C	8.012225	13.815445	-4.563465
H	6.919012	12.078084	-5.246460
C	8.754889	14.390720	-3.521427
H	9.569264	14.141912	-1.538776
H	7.840525	14.383416	-5.473437
H	9.150034	15.396269	-3.634673

## Au-BTF2

112

C	3.305882	-1.170272	0.014226
N	2.954458	-1.949348	-1.040156
N	3.064584	-1.950622	1.098232
C	2.503311	-3.188201	-0.623838
C	2.573015	-3.188913	0.729335
H	2.179521	-3.943169	-1.323340
H	2.321830	-3.944245	1.457731
C	3.287861	-1.543480	2.456707
C	4.545053	-1.786453	3.032066
C	2.236485	-0.925784	3.152258
C	4.734137	-1.380935	4.355140
C	2.479637	-0.540242	4.472445
C	3.714384	-0.763857	5.069104
H	5.697059	-1.547513	4.830612
H	1.690590	-0.053098	5.039106
H	3.883370	-0.454088	6.096937
C	5.680839	-2.443583	2.270946
C	6.154962	-3.725033	2.962841
C	6.838763	-1.462580	2.061944
H	5.309682	-2.725074	1.279346
H	5.334350	-4.440061	3.088882
H	6.939852	-4.207317	2.369176
H	6.572172	-3.515745	3.954573
H	6.501683	-0.565735	1.530450
H	7.271437	-1.148698	3.019220
H	7.634405	-1.933758	1.472921
C	0.884953	-0.654400	2.518987
C	0.643833	0.851295	2.371546
C	-0.248558	-1.326161	3.299597
H	0.887433	-1.084014	1.511178
H	1.437289	1.319116	1.778292
H	-0.314581	1.035934	1.872184
H	0.613172	1.346112	3.349493
H	-0.088990	-2.406730	3.386870
H	-0.336862	-0.917522	4.312765
H	-1.206200	-1.162018	2.792610
C	3.037932	-1.541496	-2.414177
C	1.925209	-0.913918	-2.996163
C	4.225705	-1.795404	-3.118259
C	2.032139	-0.530338	-4.334905
C	4.278805	-1.390968	-4.454031
C	3.195358	-0.764634	-5.057666
H	1.192011	-0.036720	-4.816095
H	5.185061	-1.565588	-5.027748
H	3.258301	-0.456411	-6.097850
C	5.430196	-2.459868	-2.478693
C	6.600590	-1.477217	-2.370082

C	5.838808	-3.731615	-3.227564
H	5.156656	-2.754410	-1.459491
H	6.314020	-0.588424	-1.796967
H	7.450981	-1.952466	-1.867081
H	6.937037	-1.149787	-3.360956
H	5.010164	-4.445942	-3.287123
H	6.164328	-3.509880	-4.250383
H	6.674619	-4.220292	-2.714085
C	0.648492	-0.631670	-2.226978
C	-0.561763	-1.308092	-2.877662
C	0.425954	0.875953	-2.070795
H	0.755967	-1.050907	-1.220510
H	-0.415971	-2.390282	-2.968126
H	-1.461283	-1.133866	-2.276334
H	-0.752996	-0.910708	-3.881112
H	1.277127	1.348131	-1.567917
H	0.293915	1.361150	-3.045114
H	-0.475035	1.067542	-1.476257
Au	4.036988	0.745827	-0.017290
C	4.769805	2.649747	-0.040151
C	5.073198	3.337728	1.157770
C	5.006099	3.342316	-1.248225
C	5.582898	4.634103	1.174948
H	4.904846	2.838525	2.110276
C	5.513511	4.634954	-1.249308
H	4.787738	2.853577	-2.197196
C	5.804348	5.284531	-0.038185
H	5.803496	5.125959	2.120654
C	5.831642	5.529962	-2.436920
C	6.322232	6.614563	-0.339550
C	6.347966	6.777615	-1.739417
C	6.755141	7.645125	0.494612
C	6.801411	7.954378	-2.301810
C	7.210694	8.828319	-0.073748
H	6.740840	7.532190	1.575433
C	7.240884	8.999203	-1.466256
H	6.831007	8.102066	-3.377800
H	7.549681	9.629678	0.578847
C	4.573860	5.829750	-3.283866
H	4.251005	4.887073	-3.746814
H	4.870070	6.491942	-4.109490
C	6.904688	4.905703	-3.357368
H	6.467988	4.009813	-3.819822
H	7.100430	5.610343	-4.177758
C	8.214982	4.537736	-2.673613
H	8.916302	4.104734	-3.395502
H	8.693219	5.416828	-2.228137
H	8.052808	3.802524	-1.878134
C	3.407751	6.448320	-2.523878
H	3.686151	7.409712	-2.078735
H	2.561345	6.623935	-3.197109
H	3.066372	5.789798	-1.717931

C	7.718996	10.235416	-2.079739
N	7.786511	10.431131	-3.361927
S	8.258074	11.603706	-1.087919
C	8.272711	11.682201	-3.659139
C	8.594559	12.489067	-2.544157
C	8.462968	12.188911	-4.951201
C	9.097218	13.779963	-2.696663
C	8.963007	13.472718	-5.103815
H	8.215937	11.568238	-5.807055
C	9.277260	14.262027	-3.987431
H	9.341760	14.393144	-1.834589
H	9.114113	13.874899	-6.101610
H	9.667776	15.265472	-4.131398

## IV. X-ray Crystallography

### Single Crystal Structure Determinations:

Single crystal data for Au-BTF0, Au-BTF1 and Au-BTF2 were collected using a Bruker Quest diffractometer with a fixed chi angle, a sealed tube fine focus X-ray tube, single crystal curved graphite incident beam monochromator, a Photon100 CMOS area detector and an Oxford Cryosystems low temperature device. Examination and data collection were performed with Mo K $\alpha$  radiation ( $\lambda = 0.71073$  Å) at 150 K. Data were collected, reflections were indexed and processed, and the files scaled and corrected for absorption using APEX3 [1]. The space groups were assigned and the structures were solved by direct methods using XPREP within the SHELXTL suite of programs [2] and refined by full matrix least squares against  $F^2$  with all reflections using Shelxl2018 [3] using the graphical interface Shelxle [4]. If not specified otherwise H atoms attached to carbon, boron and nitrogen atoms as well as hydroxyl hydrogens were positioned geometrically and constrained to ride on their parent atoms. C-H bond distances were constrained to 0.95 Å for aromatic and alkene C-H moieties, and to 1.00, 0.99 and 0.98 Å for aliphatic C-H, CH<sub>2</sub> and CH<sub>3</sub> moieties, respectively.  $U_{\text{iso}}(\text{H})$  values were set to a multiple of  $U_{\text{eq}}(\text{C})$  with 1.5 for CH<sub>3</sub> and 1.2 for C-H and CH<sub>2</sub> units, respectively.

For Au-BTF2 disorder is observed for solvate molecules. One benzene ring was refined as disordered over two orientations. A pentane molecule was refined as disordered with a minor benzene molecule. The two minor benzene molecules were constrained to resemble ideal hexagons with C-C bond distances of 1.39 Å. The major moieties were refined freely.  $U^{\text{ij}}$  components of ADPs for disordered atoms closer to each other than 2.0 Å were restrained to be similar. Subject to these conditions the occupancy ratios refined to 0.702(5) to 0.298(5) and 0.780(6) to 0.220(6), respectively.

Complete crystallographic data, in CIF format, have been deposited with the Cambridge Crystallographic Data Centre. CCDC 1917590-1917592 contains the supplementary crystallographic data for this paper. These data can be obtained free of charge from The Cambridge Crystallographic Data Centre via [www.ccdc.cam.ac.uk/data\\_request/cif](http://www.ccdc.cam.ac.uk/data_request/cif).

[1] Bruker (2016). Apex3 v2016.9-0, Saint V8.34A, SAINT V8.37A, Bruker AXS Inc.: Madison (WI), USA, 2013/2014.

[2] a) SHELXTL suite of programs, Version 6.14, 2000-2003, Bruker Advanced X-ray Solutions, Bruker AXS Inc., Madison, Wisconsin: USA b) Sheldrick GM. A short history of SHELX. *Acta Crystallogr A*. **2008**, *64(1)*, 112–122.

[3] a) Sheldrick GM. University of Göttingen, Germany, **2018**. b) Sheldrick GM. Crystal structure refinement with SHELXL. *Acta Crystallogr Sect C Struct Chem*. **2015**, *71(1)*, 3–8.

[4] Hübschle CB, Sheldrick GM, Dittrich B. ShelXle: a Qt graphical user interface for SHELXL. *J. Appl. Crystallogr*. **2011**, *44(6)*, 1281–1284.

### Crystal Tables:

Crystal data: JJM-1-122(AuBTF0)

Chemical formula	C <sub>42</sub> H <sub>35</sub> AuNPS
$M_r$	813.70
Crystal system, space group	Triclinic, $P\bar{1}$
Temperature (K)	150
$a, b, c$ (Å)	11.8146 (5), 12.7494 (6), 12.7733 (6)
$\alpha, \beta, \gamma$ (°)	74.285 (2), 63.823 (2), 83.926 (2)
$V$ (Å <sup>3</sup> )	1661.94 (13)
$Z$	2
Radiation type	Mo $K\alpha$
$\mu$ (mm <sup>-1</sup> )	4.57
Crystal size (mm)	0.32 × 0.26 × 0.11
Data collection	
Diffractometer	Bruker AXS D8 Quest CMOS diffractometer
Absorption correction	Multi-scan, SADABS 2016/2: Krause, L., Herbst-Irmer, R., Sheldrick G.M. & Stalke D., <i>J. Appl. Cryst.</i> 48 (2015) 3-10
$T_{\min}, T_{\max}$	0.200, 0.269
No. of measured, independent and observed [ $I > 2\sigma(I)$ ] reflections	51512, 12572, 10593
$R_{\text{int}}$	0.039
$(\sin \theta/\lambda)_{\text{max}}$ (Å <sup>-1</sup> )	0.771
Refinement	
$R[F^2 > 2\sigma(F^2)], wR(F^2), S$	0.026, 0.050, 1.02
No. of reflections	12572

No. of parameters	418
H-atom treatment	H-atom parameters constrained
$\Delta\rho_{\max}, \Delta\rho_{\min}$ (e Å <sup>-3</sup> )	2.51, -1.16

Crystal data: JJM-1-200(AuBTF1)

Chemical formula	C <sub>42</sub> H <sub>53</sub> AuNPS
$M_r$	831.85
Crystal system, space group	Triclinic, $P\bar{1}$
Temperature (K)	150
$a, b, c$ (Å)	12.5710 (8), 12.7256 (8), 13.7715 (9)
$\alpha, \beta, \gamma$ (°)	104.775 (2), 104.891 (2), 111.277 (2)
$V$ (Å <sup>3</sup> )	1829.6 (2)
$Z$	2
Radiation type	Mo $K\alpha$
$\mu$ (mm <sup>-1</sup> )	4.15
Crystal size (mm)	0.51 × 0.46 × 0.36
Data collection	
Diffractometer	Bruker AXS D8 Quest CMOS diffractometer
Absorption correction	Multi-scan, <i>SADABS</i> 2016/2: Krause, L., Herbst-Irmer, R., Sheldrick G.M. & Stalke D. (2015). <i>J. Appl. Cryst.</i> 48 3-10.
$T_{\min}, T_{\max}$	0.558, 0.747
No. of measured, independent and observed [ $I > 2\sigma(I)$ ] reflections	90033, 14030, 12735
$R_{\text{int}}$	0.031
$(\sin \theta/\lambda)_{\max}$ (Å <sup>-1</sup> )	0.772
Refinement	
$R[F^2 > 2\sigma(F^2)], wR(F^2), S$	0.022, 0.046, 1.14
No. of reflections	14030
No. of parameters	418
H-atom treatment	H-atom parameters constrained
$\Delta Q_{\max}, \Delta Q_{\min}$ (e Å <sup>-3</sup> )	4.22, -1.17

Crystal data: JJM-1-282(AuBTF2)	
Chemical formula	$C_{51}H_{56}AuN_3S \cdot 1.11(C_6H_6) \cdot 0.39(C_5H_{12})$
$M_r$	1054.85
Crystal system, space group	Triclinic, $P\bar{1}$
Temperature (K)	150
$a, b, c$ (Å)	14.8591 (8), 15.9180 (8), 24.8004 (14)
$\alpha, \beta, \gamma$ (°)	91.478 (2), 98.399 (2), 114.388 (2)
$V$ (Å <sup>3</sup> )	5261.1 (5)
$Z$	4
Radiation type	Mo $K\alpha$
$\mu$ (mm <sup>-1</sup> )	2.88
Crystal size (mm)	0.48 × 0.46 × 0.22
Data collection	
Diffractometer	Bruker AXS D8 Quest CMOS diffractometer
Absorption correction	Multi-scan, <i>SADABS</i> 2016/2: Krause, L., Herbst-Irmer, R., Sheldrick G.M. & Stalke D., <i>J. Appl. Cryst.</i> 48 (2015) 3-10
$T_{\min}, T_{\max}$	0.532, 0.747
No. of measured, independent and observed [ $I > 2\sigma(I)$ ] reflections	127152, 39788, 30231
$R_{\text{int}}$	0.041
$(\sin \theta/\lambda)_{\text{max}}$ (Å <sup>-1</sup> )	0.772
Refinement	
$R[F^2 > 2\sigma(F^2)], wR(F^2), S$	0.035, 0.095, 1.04
No. of reflections	39788
No. of parameters	1270
No. of restraints	294
H-atom treatment	H-atom parameters constrained
$\Delta\rho_{\text{max}}, \Delta\rho_{\text{min}}$ (e Å <sup>-3</sup> )	2.80, -2.00

## V. References

- 
- <sup>1</sup> Partyka, D. V.; Robilotto, T. J.; Zeller, M.; Hunter, A. D.; Gray, T. G. *Organometallics* **2008**, *27*, 28–32.
- <sup>2</sup> Gaussian 16, Revision A.03, Frisch, M. J.; Trucks, G. W.; Schlegel, H. B.; Scuseria, G. E.; Robb, M. A.; Cheeseman, J. R.; Scalmani, G.; Barone, V.; Petersson, G. A.; Nakatsuji, H.; Li, X.; Caricato, M.; Marenich, A. V.; Bloino, J.; Janesko, B. G.; Gomperts, R.; Mennucci, B.; Hratchian, H. P.; Ortiz, J. V.; Izmaylov, A. F.; Sonnenberg, J. L.; Williams-Young, D.; Ding, F.; Lipparini, F.; Egidi, F.; Goings, J.; Peng, B.; Petrone, A.; Henderson, T.; Ranasinghe, D.; Zakrzewski, V. G.; Gao, J.; Rega, N.; Zheng, G.; Liang, W.; Hada, M.; Ehara, M.; Toyota, K.; Fukuda, R.; Hasegawa, J.; Ishida, M.; Nakajima, T.; Honda, Y.; Kitao, O.; Nakai, H.; Vreven, T.; Throssell, K.; Montgomery, J. A., Jr.; Peralta, J. E.; Ogliaro, F.; Bearpark, M. J.; Heyd, J. J.; Brothers, E. N.; Kudin, K. N.; Staroverov, V. N.; Keith, T. A.; Kobayashi, R.; Normand, J.; Raghavachari, K.; Rendell, A. P.; Burant, J. C.; Iyengar, S. S.; Tomasi, J.; Cossi, M.; Millam, J. M.; Klene, M.; Adamo, C.; Cammi, R.; Ochterski, J. W.; Martin, R. L.; Morokuma, K.; Farkas, O.; Foresman, J. B.; Fox, D. J. Gaussian, Inc., Wallingford CT, 2016.
- <sup>3</sup> Dolg, M.; Wedig, U.; Stoll, H.; Preuss, H. *J. Chem. Phys.* **1987**, *86*, 866–872.
- <sup>4</sup> Perdew, J. P.; Burke, K.; Ernzerhof, M. *Phys. Rev. Lett.* **1996**, *77*, 3865–3868.
- <sup>5</sup> Godbout, N., Salahub D. R.; Andzelm J.; Wimmer, E. *Can. J. Chem.* **1992**, *70*, 560–571.
- <sup>6</sup> Miertus S. ; Scrocco E. ; Tomasi, J. *Chem. Phys.* **1981**, *55*, 117–129.
- <sup>7</sup> Tomasi J.; Mennucci, B.; Cammi, R. *Chem. Rev.* **2005**, *105*, 2999–3093.
- <sup>8</sup> Cancès E.; Mennucci, B.; Tomasi, J. *J. Chem. Phys.* **1997**, *107*, 3032–3041.
- <sup>9</sup> Mennucci, B.; Cancès, E.; Tomasi, J. *J. Phys. Chem. B* **1997**, *101*, 10506–10517.
- <sup>10</sup> Gorelsky, S. I. AOMix: Program for Molecular Orbital Analysis; University of Ottawa, version 6.94, 2018, <http://www.sg-chem.net>.
- <sup>11</sup> Gorelsky, S. I.; Lever, A. B. P. *J. Organomet. Chem.* **2001**, *635*, 187–196.
- <sup>12</sup> A. V Nikolaitchik, O. Korth and M. A. J. Rodgers, *J. Phys. Chem. A*, 1999, **103**, 7587–7596.
- <sup>13</sup> K. Suzuki, A. Kobayashi, S. Kaneko, K. Takehira, T. Yoshihara, H. Ishida, Y. Shiina, S. Oishi and S. Tobita, *Phys. Chem. Chem. Phys.*, 2009, **11**, 9850–9860.
- <sup>14</sup> A. M. Brouwer, *Pure Appl. Chem.*, 2011, *83*, 2213.
- <sup>15</sup> U. Resch-Genger and K. Rurack, *Pure Appl. Chem.*, 2013, *85*, 2005–2013.
- <sup>16</sup> M. Montalti, A. Credi, L. Prodi and M. Teresa Gandolfi, *Handbook of Photochemistry, Third Edition*, CRC Press, 3rd Edition., 2006.
- <sup>17</sup> F. Wilkinson, W. P. Helman and A. B. Ross, *J. Phys. Chem. Ref. Data*, 1993, **22**, 113–262.
- <sup>18</sup> I. Carmichael and G. L. Hug, *J. Phys. Chem. Ref. Data*, 1986, **15**, 1–250.
- <sup>19</sup> C. Creutz, M. Chou, T. L. Netzel, M. Okumura and N. Sutin, *J. Am. Chem. Soc.*, 1980, **102**, 1309–1319.

---

<sup>20</sup> R. L. Sutherland, *Handbook of Nonlinear Optics*, CRC Press, Second Edi., 2003.

<sup>21</sup> T. N. Singh-Rachford and F. N. Castellano, *Coord. Chem. Rev.*, 2010, **254**, 2560–2573.